ANTIMICROBIAL POLYMER COMPOSITES FOR MEDICAL APPLICATIONS

KTH Chemical Science
and Engineering

PETER KAALI

Doctoral Thesis

Stockholm, Sweden 2011

AKADEMISK AVHANDLING

Som med tillstånd av Kungliga Tekniska Högskolan i Stockholm framlägges till offentlig granskning för avläggande av teknisk doktorsexamen Fredagen den 13 Maj 2011, kl. 13.00 i sal F3, Lindstedtsvägen 23, KTH, Stockholm. Avhandlingen försvaras på engelska.

Contact information:

KTH Chemical Science and Engineering
Department of Fibre and Polymer Technology
Royal Institute of Technology
Teknikringen 56-58
SE-100 44 Stockholm
Sweden

Printed by AJ E-print AB
Stockholm, Sweden, 2011

TRITA-CHE-Report 2011:19
ISSN 1654-1081
ISBN 978-91-7415-899-1
www.kth.se

To My Family

ANTIMICROBIAL POLYMER COMPOSITES FOR MEDICAL APPLICATIONS
PETER KAALI

Department of Fibre and Polymer Technology
Chemical Science and Engineering
Royal Institute of Technology (KTH)
SE-100 44 Stockholm, Sweden

ISBN 978-91-7415-899-1, ISSN 1654-1081, TRITA-CHE-Report 2011:19

ABSTRACT

The current study and discuss the long-term properties of biomedical polymers in vitro and in vivo and presents means to design and manufacture antimicrobial composites. Antimicrobial composites with reduced tendency for biofilm formation should lead to lower risk for medical device associated infection.

The first part analyse in vivo degradation of invasive silicone rubber tracheostomy tubes and presents degradation mechanism, degradation products and the estimated lifetime of the materials.. It was found that silicone tubes undergo hydrolysis during the long-term exposure in vivo, which in turn results in decreased stability of the polymer due to surface alterations and the formation of low molecular weight compounds.

The second part of the study presents the manufacturing of composites with single, binary and ternary ion-exchanged zeolites as an antimicrobial agent. The ion distribution and release of the zeolites and the antimicrobial efficiency of the different systems showed that single silver ion-exchanged zeolite was superior to the other samples. Antimicrobial composites were prepared by mixing the above-mentioned zeolites and pure zeolite (without any ion) with different fractions into polyether (TPU), polyether (PEU) polyurethane and silicone rubber. The antimicrobial efficiency of binary and ternary ion-exchanged samples was similar which is thought to be due to the ion distribution in the crystal structure.

The changes in the mechanical and surface properties of the composites due to the zeolite content demonstrated that the increasing zeolite content reduced the mechanical properties while the surface properties did not change significantly. The antimicrobial tests showed that the silver-containing composite was the most efficient among all the other samples. The binary and ternary ion-exchanged composites expressed similar antimicrobial efficiency as it was seen previously for the different zeolite systems. Biocompatibility was studied by exposure to artificial body fluids to simulate the degradation of the composites in the human

body. Significant changes were observed in the morphology, the surface properties and the chemical structure.

Key Words: antimicrobial, ion-exchanged zeolite, in vitro, in vivo test, polyurethane, silicone rubber, degradation, medical polymers

LIST OF PAPERS

This Doctoral thesis is based on the following papers:

I. Degradation of Biomedical Polydimethylsiloxanes During Exposure to In Vivo Biofilm Environment Monitored by FE-SEM, ATR-FTIR, and MALDI-TOF MS
Peter Kaali, Dane Momcilovic, Agneta Markström, Ragnhild Aune, Gyorgy Czel, Sigbritt Karlsson
Journal of Applied Polymer Science, Vol. 115, 802–810 (2010)

II. Antimicrobial properties of Agþ loaded zeolite polyester polyurethane and silicone rubber and long-term properties after exposure to in-vitro ageing
Peter Kaali, Emma Strömberg, Ragnhild Aune, Gyorgy Czel, Dane Momcilovic, Sigbritt Karlsson
Polymer Degradation and Stability, Vol. 95, 1456-1465, (2010)

III. Modelling the ion distribution in single, binary and ternary ion exchanged A zeolite
Peter Kaali, Emma Strömberg, Ragnhild Aune, Sigbritt Karlsson, Gyorgy Czel
Submitted to Microporous and Mesoporous Materials, March 2011

IV. The influence of Ag^{+}, Zn^{2+} and Cu^{2+} exchanged zeolite on antimicrobial and long term in vitro stability of medical grade polyether polyurethane
Peter Kaali, Maria M. Peréz-Madrigal, Emma Strömberg, Ragnhild Aune, Sigbritt Karlsson, Gyorgy Czel
Submitted to Express Polymer letters, March 2011

V. Prevention of Biofilm Associated Infections and Degradation of Polymeric Materials used in Biomedical Applications
Peter Kaali, Emma Strömberg, Sigbritt Karlsson,
Biomedical Engineering,Trends, Researches and Technologies, Intech Open Access Publishing, 513-540, (2011)

TABLE OF CONTENTS

1 PURPOSE OF THE STUDY

The overall themes for the thesis were the long-term properties of biomedical polymeric materials and means to design new biomedical composites demonstrating antimicrobial properties. The objectives of the thesis were to present and discuss:

- the chemical, physical and mechanical changes after *in vivo* degradation of invasive silicone rubber tracheostomy tubes
- the degradation mechanisms and degradation products in *in vivo* degraded silicone rubber tubes
- the possibility to prepare antimicrobial zeolites by ion-exchange
- the antimicrobial efficiency of single, binary and ternary ion exchanged-zeolites that contain the variations of silver, copper and zinc ions
- the manufacturing of antimicrobial polyurethane and silicone rubber composites by the use of ion loaded zeolites
- the antimicrobial, mechanical, surface and chemical properties of the composites
- the alteration of surface morphology, properties and chemical structures in composites during exposure to simulated human environment using artificial body fluids as a biocompatibility test

.

2 INTRODUCTION

Polymers have a wide variety of applications in the medical industry. The most important of these are those that are used as internal or partly internal (invasive) devices, where the polymer is in contact with the human body. For biomedical applications polymers need to meet certain requirements and regulations in order to be safely used inside the human body. First of all they need to be biocompatible, neutral to the human body and have excellent stability and resistance to tissues, cells, enzymes and different kinds of bodily fluids. The biocompatibility of polymers depends not only on their chemical structure, but is highly influenced by several other factors. The body`s response to a polymeric medical device can be acceptance or rejection which depends on the location and movement of the material and the surrounding human environment as well. The microbiological effect and biofilm formation on the internal medical devices are also of great importance for the material performance. If biofilm formation initiates on the surface it can initiate degradation processes. The capability of microbes to adhere to a certain polymer and initiate degradation inside the human body is highly structure dependant. Once degradation initiates, along with the migration of additives and low molecular weight compounds, the polymer loses its biocompatibility and stability, which can lead to the failure of the device and/or cause health related issues. Therefore, an understanding of the different degradation processes that may occur inside the human body due to blood, tissue or biofilm interactions are very important. Apart from degradation, the high concentration of microorganisms in the biofilm can also cause serious infections and health related issues. Therefore, for biomedical applications the selection of the right polymers that express high stability against the previously mentioned factors is essential.

2.1 BIOCOMPATIBILITY

By definition the biocompatibility of a medical device or implant is the ability of the material to perform without causing a host response, or having toxic or injurious effects. Biocompatibility is the basic requirement of implantable materials and it plays a very important role throughout the lifetime of the biomedical device [1-3]. A non-biocompatible implant is rapidly encapsulated by collagen tissue, resulting in failure of the desired function of the product which may in turn cause serious problems. The amount of tissue growth around the material depends on the polarity; non-polar polymers are surrounded by less tissue, than polar polymers[3]. If the body`s response is rejection of a certain material, the body tries to expel it through chemical reactions by phagocytic or enzymatic activity [3, 4], resulting in the emergence of inflammations. This bodily response is highly dependent on the form (foam, fibre, film), shape, and movement of the implant, as well as the location in the body. A

smooth, rounded shape presents less interaction and reduces tissue adhesion around the material as compared to a rough-edged shape. Polymer powders give extremely high tissue interactions due to large specific surface areas [3]. Adsorption of various bodily chemicals (e.g. triglycerides and steroids) by the material can alter polymer properties and also lead to degradation [4].

Every polymeric material degrades to a certain extent upon contact with the human environment. Even under normal circumstances polymer implants undergo abrasion and are subjected to different stresses [5]. Poor long-term properties such as low wear resistance and mechanical stress results in the displacement of the implant, which is indicated as discomfort or pain by the patient.The device or implant must be non-harmful during interactions with tissues and no toxic substances may be formed or leach out during the implementation of the application. Biomedical materials must be non-toxic, non carcinogenic, non-thrombogenic, non-inflammatory and non-immunogenic [6, 7]. Low molecular weight additives and degradation products produce significant tissue interactions due to their mobility and solubility in bodily chemicals. Therefore, polymers that contain leaching additives, residual monomers and polymerisation catalysts are usually not suitable for implant purposes (REF).

Due to the constant blood exposure, extracorporeal devices are usually required to be biocompatible with blood to reduce the probability of clogging during the use. Therefore, the surface treatment of these biomedical devices is essential. It is usually achieved by applying anticoagulants (e.g. heparin). Only a few polymeric materials have good blood compatibility; hydrogels, polyether urethane ureas, and materials produced by affixing biologically inactivated natural tissue to the polymer surface [3].

2.2 BIOCOMPATIBLE POLYMERS IN MEDICAL APPLICATIONS

The most commonly used polymer materials for biomedical applications are polyurethanes, polyolefins, silicones, fluoropolymers, vinyl- and acrylic polymers. Polyether type polyurethanes are used in a variety of applications (ligament replacements, heart valve prostheses, vascular graft prostheses, breast prosthesis, catheter, cannulae etc.) due to its good biocompatibility, high resistance against hydrolysis and body fluids, excellent mechanical properties (high tensile strength, highly elastomeric) and low degree of degradation. The application of this polymer is versatile and covers a broad range from foam to film, as well as gel and bulk materials [3].

Silicone rubber is a medical elastomer (poly(dimethyl siloxane)), and is as prevalent and versatile as polyurethanes. This polymer can be synthesized in a very pure form, which makes it highly inert and results in excellent chemical resistance (due to the high hydrophobicity). Besides poly(dimethyl siloxane), vinyl- and aromatic (phenyl) dimethyl siloxanes are used

preferably as medical polymers due to their superior surface properties (e.g. super hydrophobicity). This surface characteristic as well as the aromatic groups in the structure make silicone rubbers´ surface less attractive to microorganisms, thus avoiding biofilm formation. These polymers are used in artificial skin, joint replacement, vitreous replacement, artificial heart, breast implants, different types of catheters and cannulae production [3].

Polyolefins (polyethylene, polypropylene), fluoropolymers (teflon) and acrylic polymers are mostly used as prosthetic devices. They express high degrees of biocompatibility (almost neutral), excellent chemical resistance and superior mechanical properties. Compared to metallic implants the main advantage of polyolefins and fluoropolymers is the low friction coefficient and wear resistance due to their self-lubricating characteristics. The main medical applications are hip joints and knee implants [3]. Acrylic polymers show even better mechanical properties than polyolefins and they are mostly used as dental materials or bone cement to anchor artificial joints to the body. Owing to their excellent optical properties methacrylates are also used in contact lens manufacturing.

Polymers such as poly(vinyl chloride) (PVC), poly(lactic acid) (PLA), polycaprolactone (PCL) and poly(vinyl alcohol) (PVA) have a variety of different medical applications. PVC is commonly used for lung bypass sets, catheters and cannulae, tubing for dialysis and endotracheal feeding. PVC is used preferably, since it is simple to sterilize it or process it into products that do not crack or leak.

2.3 BIOFILM CHARACTERISTICS AND FORMATION

Biofilm formation on polymeric medical devices is a serious issue. By definition, biofilms are aggregates of microorganisms, which are formed due to the attachment of cells to each other and/or to a host surface in an aqueous environment [8]. In general, biofilms can host microorganisms such as bacteria, fungi, protozoa, algae and their mixtures, and usually the constituent cells require similar conditions to initiate and progress the cell growth. The factors that influence the biofilm formation are humidity, temperature, pH of the environment or medium, atmospheric conditions and nutrition sources. Besides microorganism cells, biofilms usually contain 80-90% water and depending on the host surface their thickness may vary between 50-100 m [9].

Biofilm formation starts with the deposition of microorganisms on the surface of the material, followed by growth and spreading of the colonies. Microbial colony numbers are often very high and the emerging biofilms contain several layers of microorganisms, resulting in a highly complex structure [10]. The microbial cells are encased in an adhesive matrix produced by the microorganisms of the biofilm, called extracellular polymer substance or exopolysaccharide (EPS), which contains proteins, nucleic acids, lipids and polysaccharides [11, 12]. EPS

influences the adhesion of the biofilm to the surface and plays an important role in the protection of the biofilm from the outer environment. Therefore, the biofilms have an improved resistance against toxins, detergents and antimicrobial agents. In some cases the resistance of bacterial biofilms against antibiotics can be increased by 1000 fold compared to isolated colonies.

2.3.1 Biodeterioration of polymeric materials

Biofilm formation is common on most polymeric materials used in different environments (i.e. outdoor insulators, medical catheters) with high humidity. The nutrition sources necessary for successful colonisation may consist of the material itself or a variety of pollutants that end up on the surface of the material. The biofilm-polymer interactions depend on several factors, which can be evaluated separately and in various combinations in authentic artificial environments that simulate the material's end-use conditions [13, 14].

For polymers, biodegradation is usually a complex process, starting with consumption of accessible additives and propagating with the decomposition of the matrix (Fig.1)[10].Although biofilm formation does not always lead to the biodegradation of the polymer, it can result in the loss of functionality. Through biofouling, the spreading of the biofilm over the surface, the original properties of the material such as hydrophobicity may be altered. Deterioration of the medical function by clotting and disruption of the flow, through for example a urinal catheter, may cause pain for the patient or result in a serious infection. Medical implants are convenient surfaces for microbial growth, in both short-term devices (urinary catheters) and long-term implants (artificial joints). Biofilms consist of various bacterial strains that are protected from attack by the immune system, antibiotics and other antimicrobial agents due to difficulties in penetrating into the biofilm.

Plastic materials usually contain additives, low molecular weight compounds, and residues of the polymer synthesis as well as shorter chains resulting from the degradation of the material, which can migrate out of the material and interact with the biofilm. It is known that fillers such as polyesters, adiapates, epoxidised fatty acids, oleates, stearates and carbon-based plasticisers are perfect sources of nutrition for microorganisms in the biofilm [10, 15]. The most disputed material in biomedical applications is PVC, widely used for tubing purposes. During service life, toxic phthalate plasticisers tend to migrate out of the polymer, exposing the patient and providing nutrition to a growing biofilm. This indicates that the material becomes harder and more brittle, still non-susceptible to biodegradation but instead sensitive to physical degradation.

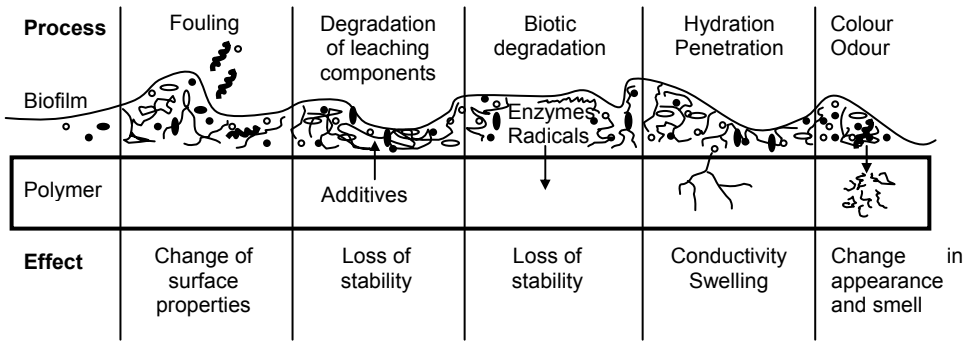

Figure 1. *Effect of biofilm formation on polymer material surface (redrawn from [9]).*

Factors influencing the rate of biodegradation are pH, environment, oxygen, salts, redox potential and temperature. Salts can be formed by anions which could be the final products of microbial metabolism and react with cations[16]. An increase in salt concentration or significant change in pH assists significantly in the breakdown of the polymer [17].

The excretion of enzymes from microorganisms may accelerate material degradation. Microorganisms are capable of causing enzymatic degradation of the polymer, which is in fact the main biodegradation mechanism for several medical polymers (e.g. polyurethane) [18, 19]).

The microorganisms in the biofilm may cause a discolouration of the polymer surface, through diffusion of lipophilic pigments into the material. These substances do not alter the properties of the polymer, but are impossible to remove [10]. The discolouration can also be caused by other environmental factors such as oxidation of filler, additives or the polymer itself[16]. Another concern during biodegradation is the formation of low molecular weight compounds, which may cause various odours. In a biomedical context the main issue is the potential harmful effects such compounds may have on the patient.

2.4 DEGRADATION MECHANISMS OF MEDICAL POLYMERS

Besides biofilm and biodeterioration, the human body itself may cause degradation of the polymer since it contains a variety of enzymes and chemicals that are capable of attacking the material[20, 21]. Polymers containing ester or amide linkages (i.e. polyurethane) are more likely to hydrolyze or oxidize, while polyether type polymers are more stable, showing minimal degradation during long-term exposure to the human body environment. Chain-scission and/or cross-linking occurs in addition to hydrolytic degradation [22].

As previously discussed, biofilm attachment to the surface of the polymeric materials plays a vital role in the initiation and propagation of the degradation process. Biofilm formation is more pronounced for invasive materials; however, implants after their implantation are rarely exposed to such aggressive biological milieus. However, the biofilm itself can cause immunological responses (i.e. infections) that change the surrounding body environment resulting in a negative effect on the material properties [23].

Based on the molecular, chemical and mechanical interactions with the human body environment, four types of degradation mechanisms of polymers used in medical applications can be distinguished: hydrolysis, oxidation, enzymatic- and physical degradation [24].The kinetics of each process differ, the key factors are the structure of the material and the surrounding environment [25]. Bodily fluids represent the environment of the given location in the body or liquids (enzymes) produced by the body as an immunological response. In this case, the important factor in the material degradation is the change of pH of the surrounding environment, since some polymers (i.e. polyesters, polyamides) are highly pH sensitive [20, 25]. Another significant factor is the water uptake of the material (which is highly dependent on the hydrophobicity).The adsorbed water acts as a plasticizer, altering the physical properties of the material. It may also swell the polymer, causing dimensional instability of the device or implant and initiating the degradation of the polymer through hydrolysis.

2.4.1 Hydrolysis

In general, hydrolysis of polymers occur in three stages, however, depending on the molecular weight and the type some polymers undergo only one or two stages [24]. In the first stage, the polymer adsorbs water and becomes saturated in a short period of time, thereafter reactions between the water molecules and the polymer chains initiate. At this stage no auto-acceleration occurs since the water content of the polymer is constant, the molecular weight is high and the chain-end concentration is low. This is followed by the second stage, where the molecular weight of the polymer decreases and the chain-end concentration increases to a critical level whereupon auto-acceleration initiates and catalyzes the degradation process. The increase in the chain-end concentration leads to an increase in the water adsorption of the polymer extending the polymer-water interactions. This results in a further decrease in the molecular weight. At a certain point the molecular weight becomes so low that it becomes soluble in the media. This corresponds to stage three. The low molecular weight compounds that form due to the reactions dissolve in the media and the molecular weight of the polymer gradually decreases until the polymer is completely dissolved. Although the water uptake of medical polymers is low (i.e. polyesters ~1%), hydrolysis and bond-cleavage within the polymer chain result in a material with a decreased molecular weight and increased number of

hydrophilic chain-ends. The chain-ends may adsorb an increasing amount of water which can further catalyze the reaction and lead to the complete breakdown of the material.

This is the typical degradation mechanism for polyesters, polyamides and polycarbonates, however, the hydrolytic degradation of the stable poly(dimethylsiloxane) may also occur during *in vivo* use [22, 26]. The hydrolysis of the silicone rubber initiates with bond-scission of the methyl groups of the cross-links and on the backbone of the polymer. This results in the formation of a series of low molecular weight compounds (both linear and cyclic) that can migrate out of the material and cause toxicity.

2.4.2 Oxidative degradation

The oxidative degradation of medical polymers occurs inside the human body and can be monitored in simulated environments [27, 28]. The reaction is caused by the peroxides produced by the human body against "non-accepted" implant materials through a rejection mechanism [24, 29]. Inflammation takes place at the implantation site, where monocytes migrate to the site and the production of macrophages may initiate. If rejection is not possible, the body tries to encapsulate the material via foreign body giant cells. These cells and macrophages produce peroxides in order to try to break down the material and eliminate it from the body [24]. The oxidation mechanism begins with an increasing number of free radicals due to the oxygen adsorbed from the surrounding tissues or blood. The oxygen molecules react with the existing free radicals [24], resulting in an accelerated process where each oxygen molecule produces two radicals. The newly formed free radicals are transported to different parts of the polymer chain causing chain scission and the formation of new chain-ends, one carrying a free radical and the other containing a double bond. The double bond chain end can react further and form acids and ketones, while the free radical end continues the previously mentioned process. This reaction propagates until the chains become too short for further degradation. The most susceptible medical polymers for oxidation are polyolefins, vinyl polymers, polyethers and polyamides. However, several studies have confirmed that polyether type polyurethanes are quite stable against hydrolysis without exposure to oxidation [29-31]. The oxidative degradation takes place primarily at the ether linkage of the polymer, where the peroxide radical attacks the carbon of the soft segment. This reaction leads to the formation of an ester linkage, which is susceptible to hydrolysis. The oxidative degradation of polyether urethane is therefore followed by hydrolysis. The polymeric materials that are susceptible or less susceptible to certain degradation processes are summarized in Table 1.

Table 1. *Polymeric materials susceptible to degradation.*

Degradation	Susceptible	Less susceptible
Hydrolysis	Polyanhydride Polyorthoester Polyketal Polyester (aliphatic)	Polyolefin Polyether Polysulfone PDMS Polycarbonate Polyimide Polyurethane Polyester (aromatic) Polyamide
Oxidation	Polyolefins Vinyl polymers Polyethers Polyamines	Fluoropolymers Polyesters Methacrylates Silicone Polysulfone Polyether ether ketone

2.4.3 Enzymatic degradation

In the human body, materials may also undergo enzymatic degradation [32-35]. This is also a defensive response of the body against implant materials and can be linked to tissue and cell activity. Although enzymes are produced for specific interactions, they are capable of recognizing "unnatural" substrates such as polymers [29].

In order to interact with the polymer, the enzyme must diffuse into the material either by swelling or hydrolysis [33]. This is considered to be the primary contact between the enzyme and the polymers´ surface. At this stage the enzyme becomes inactive, forming an "enzyme-bond" complex by attaching to an enzymatically susceptible bond (i.e. urethane, ester etc.). If this complex is relatively stable, bond scission may occur between the interface bonds and the bound enzyme, which results in the formation and release of low molecular weight compounds. These compounds then undergo further degradation and cleavage.

Table 2. *Polymers susceptible to enzymatic degradation* [34].

Polymer	Enzyme
Polyurethanes	Cholesterol esterase, xanthine oxidase, cathepsin B, collagenase
Polyglycolic acid	Esterase, chymotrypsin, trypsin
Polyester	Esterase
Polyester urea	Urease, pepsin, chymitrypsin
Polycaprolactone	Lipase, carboxytic esterase
Polyamide Polymethylmethacrylate	Esterase, papain, trypsin, chymotrypsin

Two kinds of enzymatic degradation can be distinguished; oxidation or hydrolysis of the material based on the type of the enzyme produced [18]. The enzymatic systems are highly specific and they are able to catalyze degradation of the particular polymer chains. Various enzyme systems for different polymers are summarized in Table 2.

2.4.4 Effects of sterilization on polymer degradation

During the manufacturing process biomedical materials are exposed to microorganisms and other substances even in a very clean production environment. Therefore, these products have to be sterilized and well sealed for storage in order to avoid any contamination or microbes that may cause infections or health problems right after the implantation. The sterilization procedures are presented in Figure 2.

Dry heat and autoclaving involve high temperature (~120-180 ^{o}C) and pressure and is not used for polymeric medical devices due to the risk of thermal degradation. The commonly used sterilization methods for these materials are irradiation or the use of gaseous chemicals (ethylene oxide).

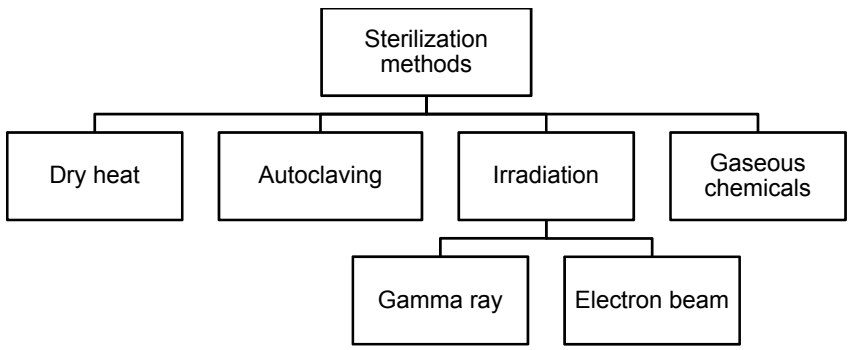

Figure 2. *Sterilization methods of medical polymers.*

There are two types of irradiation processes; gamma ray and electron beam. Both have such a high energy that the microorganisms, which remain in the material after the production, are destroyed. However, these high-energy impacts may initiate changes in the chemical structure that manifest as bonds scission, cross-linking, branching and degradation of additives. As an example, polyurethane catheters treated with electron beam sterilization undergo oxidative degradation, which leads to chain scission in the hard and soft segments. This leads to the formation of smaller highly volatile soft segmental fractions. Additionally in case of polymers e.g. polyurethane, cross-linking may occur due to the chain scission of the hard segment. These chain scissions initiate the formation of urethane linkage sites. Furthermore, most of the medical polymers contain additives that can be degraded by the electron beam and therefore

easily released from the polymer. This results in decreased stability of the polymer and may cause cytotoxicity[36-40]. Gamma irradiation has a similar influence on polymers. Due to the gamma sterilization, branching and oxidation of polyurethanes occur [41].

Besides the type of irradiation, the dosage, flux and the outer environment have an effect on structural changes during the sterilization (e.g. the higher flux and the presence of oxygen increases the oxidation).

Besides irradiation, the use of gaseous chemicals is also prevalent. For this purpose ethylene oxide is usually used as it is a strong alkylating agent, toxic and carcinogenic gas. The effectiveness of this gas on sterilization depends on the sterilization method which includes several factors. These are regarded as the gas concentration, temperature, relative humidity, the permeability and absorbance of the polymer. Sterilization with ethylene oxide has no or minimal influence on the structure of the polymer [42-45]. However, the residues of the gas that remain after the process could cause toxicity at a certain concentration (above 400 ppm) [46, 47]. In principle the amount of remaining residue depends on the applied sterilization method and the polymer`s absorbance. Therefore, proper method development allowing the complete release of ethylene oxide from the polymer structure is necessary.

2.4.5 Effects of degradation products on the human body

The degradation of the biomedical materials and formation of the degradation products have a serious influence on the human body [24]. For instance, due to hydrolysis carboxylic acid and/or hydroxyl chain ends may form. Hydroxyl groups can be further oxidized and the reaction may produce different kinds of degradation products i.e. aldehydes, ketones or carboxylic acids. The degradation rate and its influence on the body depend on the size and location of the implant. However, if a biocompatible material starts to degrade it loses its stability and from an application point of view it causes decreased service time. An example for body reaction is the formation of carboxylic acid, which changes the local pH, causing an inflammatory response. For example during the production of some polyurethanes, methylene diamine is used, which is a toxic compound. In the case of these kinds of toxic precursors biodegradation is not relevant since base monomer usually does not form due to chemical degradation. However, residues of these monomers may remain in the material after production. This is a technological question and the ability of the human body to handle these kinds of compounds depend on several factors i.e. can the compound be diluted or transported to organs (i.e. kidney) where it can be further degraded or flushed away [21].

2.5 PREVENTION OF BIOFILM FORMATION AND RELATED INFECTIONS

The potential risk of biofilm formation is a big problem influencing the degradation of invasive materials and may cause health related issues. Patients often face catheter associated infections (CAI) [48]. From a medical point of view, depending on the type of catheter (central venous, urinary etc.), the infection might be lethal for the patient. For the hospitals, these infections appear as a cost increase for patient therapy, which might be anticipated if the biofilm can be properly removed from the surface of the device. Currently used medical devices that are effective against microorganisms contain either biocides or silver. It is known from ancient times that silver has good antimicrobial efficiency; however, the mechanism is not fully understood. Silver ions have the capability to be exchanged by ions that exist in the environment (Ca^+, Zn^+ etc.) and attach to bacterial cells [49]. It forms chelate-complexes with the DNA of the bacteria. These complex molecules block the main transport processes of the cell, which lead to its decay. By increasing the silver ion concentration the antimicrobial activity can be increased, however, a certain concentration in the human environment (10 mg/L ,[49]) cause cytotoxicity and may lead to argyria.

The most commonly used antibiotics for the treatment of catheters are minocycline-rifampin, piperacillin, gentamicin, and ofloxacin [24, 50-52]. As an antibacterial agent silver can be used in different forms (ion, compound, hydrogel, metallic) in medical devices. The most common ones for invasive materials are chlorohexidine-silver-sulfadiazine and impregnated silver or silver coating. Clinical studies showed that monociclyne-rifampin, ofloxacim and chlorohexidine-silver-sulfadiazine result in a significant decrease in the number of CAI compared to the other agents. Furthermore, silver sulfadiazine expresses a high degree of biocompatibility and applicability in the human environment [50, 51]. Impregnated silver and silver coatings are less accurate because the mechanism is based on migration and diffusion [53]. The use of hydrogels as antimicrobial agents in the medical industry is growing. Silver-hydrogels are used preferably as dressings for wound healing [54, 55], however, they show good antiseptic properties as polymer coatings on urinary catheters as well [56]. Besides silver containing coatings, it was confirmed that nitrofurazone is also an excellent antibacterial agent and reduces the risk of urinary and blood-stream infections [57].

2.5.1 Issues with silver

The different forms of application of silver as an antimicrobial and antiseptic agent for invasive materials is promising based on current experience and clinical trials, however, the real efficiency is sometimes questionable [52]. In order to use silver in medical applications, the standardization of this material is necessary. This standardization is difficult since the effect is influenced by several factors; the destruction of different bacterial strains requires different silver concentrations and the minimum inhibitory results may give broad intervals of

concentration. As an example, the minimum inhibitory concentration (MIC) for *Stapylococcusaureus* and *Pseudomonas aeruginosa* can vary 8-80 mg/L [58].This broad interval depends on the variation of the silver concentrations in different products and the variation of the release as a function of time depending on the nature of the material (i.e. water absorption) and the physical, chemical form of the silver and the location in the material. Moreover, there are bacterial strains that are resistant to silver and this mechanism is not yet well understood. There are species that become resistant by the modification of gene mutation or identification of the silver as a toxic material when it gets into the cell resulting in a rejection mechanism. Besides silver, certain bacterial strain has resistance against specific antibiotics (e.g. MRSA: Methicillin-Resistant *Staphylococcus aureus*) or in extreme cases this resistance can expand to several groups of drugs.

During the improvement and development of antimicrobial and antiseptic materials that inhibit biofilm formation and infections, these factors must be well considered.

2.5.2 Zeolites as potential antimicrobial agents

Zeolites are minerals that have a variety of natural and synthetic forms. The largest application field of these materials is in agriculture and industry where zeolites are used for water purification treatments (ion-exchange beds, filters, detergents), construction and soil treatments [59, 60]. It has been confirmed by several authors that due to the excellent ion exchange properties, zeolites adsorb heavy metals easily [61-63]. Besides industrial use, zeolites have a high importance as food supplements and agents as well as medical treatments for both humans and animals [64, 65]. Zeolites have the potential to be applied as antimicrobial agenst. This mechanism is based on the ion exchange where the ions that are incorporated in the structure exchange with other ions (i.e. Na, K etc.) that can be found in the outer environment [66]. For antimicrobial applications zeolites are usually filled with antimicrobial metallic ions (i.e. silver) that are slowly released during the entire service time. The release of ions depends on several factors (matrix, temperature, ion, humidity etc.) and is based on the outer environment. It can be relatively fast or slow which influences the antimicrobial effect as well. It was previously reported that silver-zeolite express very good antimicrobial properties [67-70]. Furthermore, the application of silver-zeolite as filler in polymeric materials has also been reported in literature. It is proved that the antibacterial activity of these polymer-based composites has been increased [71, 72]. Besides silver, there are other metallic ions (i.e. Cu, Zn) that show antimicrobial effect and can be used to treat zeolites in order to make them applicable for antimicrobial purposes [73-77].

2.5.3 Antimicrobial composites

One of the main research areas of antimicrobial medical polymers is on the development and improvement of antimicrobial polymer composites. The bases of these materials are usually biomedical polymers e.g. polyurethane, silicone rubber or PVC, which are loaded with an antimicrobial agent. For this purpose different forms of silver or other antibacterial metals are used. The antimicrobial efficiency of silver, copper and titanium nanoparticles are confirmed, however, silver is superior when compared to other metals. The antimicrobial mechanism of the nanoparticles is not known but it can be assumed that it is similar to the ions. This is due to their small size and high specific surface area, which makes them extremely reactive with the environment.

The main problem that arises during the preparation and production of composites is the aggregation of the particles. This is a big issue, since the size of the particles increases due to the aggregation, which in turn influences the diffusion and the antimicrobial properties [78, 79]. Besides the size, the shape of the nanoparticles also influences the antimicrobial properties. It has been reported that truncated cone shaped particles express better efficiency against microbial growth than the spherical ones [80]. In order to reach a homogenous dispersion of the particles by mixing, the use of a surfactant is necessary [81], which complicates the manufacturing procedure, therefore the bulk reduction of the nanoparticles is preferred in the production of polymer matrix nano-composites. In this process, the polymer is responsible for the stabilization of the nanoparticles and is performed as a two step reaction. The first step is the addition of silver or any other metallic compounds into the polymer solution (i.e. $AgNO_3$). In the second step, a reducing reagent is added to the system and the formation of nanoparticles initiates. The effectiveness of this procedure has been confirmed by several studies [82-85]. Another perspective of silver-polymer composites is the incorporation of silver ions into zeolites, which are then mixed into the bulk polymer. It is known that zeolites are a natural mineral and have a high ion-exchange capability. Research papers confirm the high efficiency of Ag-zeolite polymers against microorganisms [28, 69, 86, 87]. The efficiency is based on the silver content, which is linked to the zeolite content. The higher the zeolite-content, the better the antimicrobial efficiency. However, zeolites are hydrophilic materials, therefore they adsorbs moisture and water easily, which makes the composite more versatile against solvents and other degrading fluids.

The antimicrobial efficiency of these materials is based on the diffusion of the particles from the bulk of the polymer to the surface where the antimicrobial agent interacts with the microorganism cells. The diffusion is governed by a concentration gradient, which arises between the bulk of the composite material and the environment. In order to reach equilibrium the antimicrobial agents are concentrated on the surface and if it is possible diffuse out. This process depends on several factors including the structure of the material, temperature,

humidity etc. The main issue with these composites could be their limited antimicrobial effect. This is due to the slow diffusion of the antimicrobial agent. In contrast the slow diffusion rate ensures the continuous and even release of the agent.

3 EXPERIMENTAL

3.1 MATERIALS

3.1.1 Zeolite

A zeolite was used as an antimicrobial agent, which was filled with different metallic ions during the experiments. This type of zeolite is one of the most prevalent synthetic zeolites that crystallize in a cubic crystal-lattice. The diameter of its pores (4.2 Å) is assigned by eight tetrahedrally coordinated silicon (or aluminum) atoms and eight oxygen atoms that form rings. The main cavity in the middle of the crystal is surrounded by eight sodalite cages that are linked to each other. The diameter of this central cavity is typically 11.4 Å, the unit cell parameter is 24.61 Å and the porosity is 47 %. The Si/Al ratio in A zeolite is 1.0.

In the current study ZEOMIC AJ10D inorganic antimicrobial agent (Ag content 2.5%) was purchased from SinanenZeomic Co., Ltd. (Tokyo, Japan), which was then modified according to the experiments. The physical properties of this material are presented in Table 3.

Table 3. *Physical properties of ZEOMIC AJ10D.*

Form	White fine powder
Specific gravity	2.1 (-)
Bulk density	0.4 (g/cm^3)
Average particle size	2.5 (μm)
pH	7 - 9(g-Zeo/100ml-H_2O)
Heat resistance	800 (°C)
Acid resistance	pH3
Alkali resistance	pH13

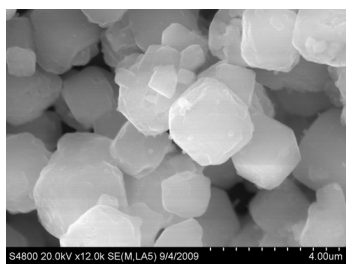

Figure 3. *SEM micrograph of the ZEOMIC AJ10D powder.*

3.1.1.1 Preparation of antimicrobial zeolite samples

The following chemicals were used for the preparation of different ion-exchanged zeolite samples: sodium chloride (puriss. p.a., ≥ 99.5 %), silver nitrate (purum p.a., crystallized, ≥ 99.0 %), zinc nitrate hexahydrate (purum, ≥ 98 %), copper nitrate trihydrate (puriss. p.a., 99-104 %) were purchased from Sigma Aldrich (Stockholm, Sweden).

Single, binary and ternary ion-exchanged zeolite samples were prepared by ion-exchange reactions. First the zeolite was saturated with sodium ions which removed the other unnecessary ions and impurities from the structure. For this purpose 1 g zeolite was added to 40 ml 1M NaCl solution. The ion exchange took place at room temperature for 24 hours under constant stirring. The solution was replaced with fresh 1M NaCl every 8 hours. Then the zeolites werebfiltered and washed 5 times with distilled water to remove the excess amount of chloride ions from the samples, and dried at 105 °C.

The second step was the preparation of single, binary and ternary ion-exchanged zeolite systems were performed. The zeolites were filled with Ag, Cu, Zn ions. In the case of binary and ternary systems a combination of these ions were applied and the preparation of the following samples were obtained: Ag-Zn, Ag-Cu, Zn-Cu, Ag-Zn-Cu. For single ion-exchanged systems 1 g zeolite was added to 40 ml 0,1M Ag-, Cu-, or Zn-nitrate solutions and the reaction took place at room temperature for 24 hours under constant stirring. In the case of binary and ternary systems the procedure was the same, where the ion-exchange reactions was performed with Ag-Zn, Ag-Cu, Zn-Cu and Ag-Zn-Cu nitrate solutions. The concentration of each component in the solution was 0.1 M. After 24 hours the zeolites were filtered, washed and dried at 105°C.

3.1.2 Silicone rubber

In the first part of the study *in vivo* tracheostomy tubes with ´Superslick´ coating made of silicone rubber were analyzed. These tubes are used for patients suffering from different respiratory disorders. The tube is inserted into the trachea right under the vocal cords in order to ensure the breathing of the patient. The tubes used in this study were purchased from Bivona TTS® and supplied by The National Respiratory Center (NRC), Danderyds hospital Stockholm, Sweden.

For the preparation of silicone rubber-zeolite composites OXAM V1 commercial silicone rubber and OXAM 40 catalyst was used that purchased from T-Silox Ltd. (Budapest, Hungary). The composites were prepared using a two-component silicone system. OXAM V1 liquid silicone rubber was mixed with 1-5 % zeolite in a beaker for 5 minutes, then 5 % OXAM 40 catalyst was added to the mixture and the mixing was continued for another 2

minutes. After that, 100x100x3 mm silicone rubber plates were casted from the mixture. The duration of the cross-linking process was 24 hours at room temperature under vacuum.

3.1.3 Polyurethane

Polyester (TPU) and polyether (PEU) type polyurethanes were used for the preparation of polyurethane-zeolite composites. Laripur 5725, polyester type thermoplastic polyurethane, was purchased from Szóradi ésTársa Ltd. (Budapest, Hungary) and BASF Elastollan 1164D50 polyether type thermoplastic polyurethane was supplied by TRACOE medical GmbH (Frankfurt, Germany). The preparation of the composites was performed according to the following procedure.

Both polyurethanes were mixed with zeolite 1-5 % of zeolite in a HaakePolylab System equipped with a Rheomix 600 mixer (Thermo Fisher Scientific Inc., Karlsruhe, Germany). In PEU, different multi-ionic zeolites were also mixed and the zeolite content in these composites was 1 %. The mixing temperature was 210 °C at 100 rpm and the duration of constant mixing was 5 minutes. After mixing the composite samples were ground into pellets and double layered samples were injection moulded from the polyester polyurethane. This process was performed in two steps on a Krauss Maffei 50-390/C1 type injection moulding machine (KraussMaffeiTechnologieGMbH, München, Germany). Pure TPU plates with a dimension of 100x100x1 mm were first injection moulded then a 0.5 mm thick zeolite-TPU layer was injected on top of the pure TPU plates. PEU composite pellets were injection moulded in only one step without any pure layer. The obtained dimensions of these samples were 100x100x1.5 mm.

3.2 TEST METHODS

3.2.1 Determination of maximum ion-exchange capacity and ion release

The maximum cation-exchange capacity (CEC) of the zeolite samples was determined for single ion systems by the Langmuir model. Different dilutions of Ag, Cu and Zn nitrate solutions were prepared with a concentration of 1, 5, 7, 10, 20, 30, 50, 70 and 100 mmol/l. 10 ml of each solution was added to 0.25 g of zeolite and was kept for 24h at room temperature under constant stirring. Then the ion-exchanged zeolites and solutions were separated by centrifugation and filtration and the remaining ion-concentration in the solutions was measured by atomic absorption spectrophotometer (AAS). The ion concentration that was transferred into the solid phase (zeolite) was calculated by the following equation:

$$q_e = (C_0 - C_e) \cdot \frac{V}{m}, \tag{1}$$

Where q_e (mmol/g) refers to the concentration of ions in the solid phase, C_0 (mmol/l) is the initial concentration and C_e (mmol/l) is the final concentration of the solution and V/m is the dilution ratio. The ion concentration of the solid phase was confirmed by Electron Dispersive X-ray Spectroscopy (EDX). Based on this the Langmuir adsorption isotherm can be drawn by the q_e-C_e function.

The maximum ion capacity that can be transferred into the solid phase was calculated using the equation of the linearized Langmuir isotherms:

$$\frac{1}{q_e} = \frac{k_L}{Q} \cdot \frac{1}{C_e} + \frac{1}{Q}, \tag{2}$$

where Q (mg/g) is the maximum amount of ions that can be transferred into the solid phase and k_L (mg/l) is a constant. By inserting a line on the $1/q_e$-$1/C_e$ function, the gradient and the intersection was determined. Based on these values the unknown components of the equation (Q, k_L) were calculated.

Similarly to the preparation of single, binary and ternary ionic zeolite systems the ion-ion release studies were based on ion-exchange reaction. The different ions in the zeolite samples were exchanged with sodium ions and the released concentration of each ion in the ion-exchange solution was measured by AAS. This experiment was performed by adding 1 g zeolite to 40 ml NaCl solutions with the following concentrations: 1, 5, 7, 10, 20, 30, 50, 70, 100 and 1000 mmol/l. The reaction was carried out for 24 hours at room temperature with constant stirring. The rate of ion release was monitored as a function of initial NaCl concentration.

3.2.2 Antimicrobial tests

The minimum inhibitory concentrations (MIC) for single, binary and ternary ion-exchanged zeolites were determined for two bacterial strains (Methicillin-resistant *Staphylococcus aureus* (MRSA) ATCC 43300, *Pseudomonas aeruginosa* ATCC 27853) and a mold *(Candida tropicalis* ATCC 90874) according to ISO 20776-1 standard test procedure. The test was carried out at 37 °C for 24 h in test tubes by adding 10 ml mixture of the inoculums and the zeolite suspension. The concentration of the inoculum in the mixture was set to $5 \cdot 10^5$ and $8 \cdot 10^6$ CFU/mL. Ten different dilutions of the zeolite were used (2, 4, 8, 16, 32, 64, 128, 256, 512 and 1028 ppm) to obtain the MIC.

Agar disc diffusion test was also carried out on the above-mentioned bacteria and mold strains according to the EUCAST standard test method to determine the inhibition zone of the

samples. Paper discs with a diameter of 6 mm were impregnated with ion-exchanged zeolites and placed on Müller-Hinton (for bacteria) or Casitone (mold) agar plates. The total zeolite content in the discs was 10 μg, the samples were incubated for 24 h at 37 °C.

The antimicrobial effect of zeolite-polymer composites was determined for the above mentioned microorganism strains according to the ISO 22196 standard. The cell concentration of the inoculum was set to $5 \cdot 10^5$ CFU/mL. The dimension of the test pieces was 50x50 mm and the duration of the test was 24 h at 37 °C.

3.2.3 In vivo test

Silicone rubber tracheostomy tubes were exposed in human patients for 1, 3 and 6 months [88]. Five patients took part in the experiment and all analytical data are presented as averages. The diagnosis and the most important details of the patients are presented in Table 4 where the unique code of each sample is also given.

Table 4. *Information on the tracheostomy tube samples and the corresponding patients.*

Patient No.	Tube No.	Gender	Diagnosis	Inhaled drugs	Note
1	SIL-205 SIL-206 SIL-208	Male	Cerebral paresis and kyphoscliosis	-	aspirate
2	SIL-209 SIL-210 SIL-212	Male	Spinal muscular atrophy	-	-
3	SIL-213 SIL-214 SIL-216	Male	Duchenne´s syndrome	-	-
4	SIL-217 SIL-218 SIL-220	Female	Stroke, COPD	Budesonide; ipratropium bromide monohydrate	+ oxygen; aspirate
5	SIL-221 SIL-222 SIL-224	Male	Stroke	-	aspirate

After the exposure, the tubes were cleaned at Danderyd Hospital, Stockholm, Sweden by the following procedure: all tubes were washed both outside and inside by soaking in warm water with perfume free detergent containing surfactants (Nilfisk-Advance, Stockholm, Sweden) and water. After that the tubes were rinsed under running water for 30 s. Finally the tubes were soaked in a disinfected cup containing 0.5 % chlorhexidine alcohol for 1 minute and then rinsed in another disinfected cup with 0.9 % sterile saline for 1 minute [88].

After the cleaning, three pieces were cut from three different areas on each tube. These areas are presented in Figure 4. Area 1 is at the neck plate where the tube penetrates into the airway.

Usually tracheostomy tubes have a fenestration in order to allow the patient to be able to talk while wearing the tube. Area 2 is at this fenestration site. Area 3 is at the end of the tube that is located the closest to the lungs. All in vivo samples were compared with a reference tracheostomy tube, which was obtained from a newly opened package.

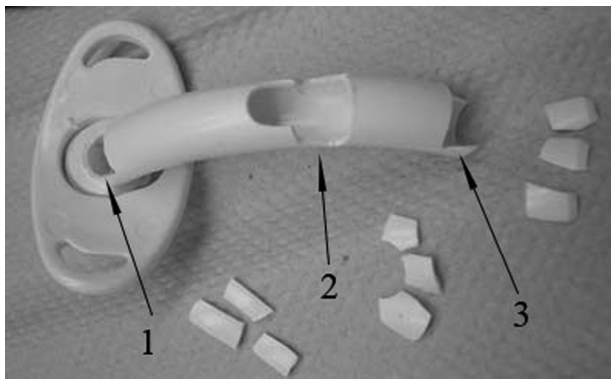

Figure 4. *The sampling areas of tracheostomy tube samples [89].*

3.2.4 In vitro test

Two synthetic body fluids were chosen to simulate different *in vivo* conditions. Both fluids have been identified to cause degradation of plastic implant materials [90, 91]. Artificial Lysosomal Fluid (ALF) simulates the immunological reaction of the body while the Gamble's solution is similar to the interstitial fluid of the deep lung. For the preparation of the artificial body fluids the following chemicals were used: sodium sulphate (purum, anhydrous, ≥ 99 %), magnesium chloride (purum, anhydrous, ≥ 98.0 %), sodium chloride (purum p.a., ≥ 99.5 %), sodium hydroxide (purum p.a., ≥ 97.0 %), sodium phosphate dibasic (purum p.a., anhydrous, ≥ 98.0 %), potassium chloride (puriss. p.a., ≥ 99.5%) and calcium chloride dihydrate (purum p.a., 99-103 %) were purchased from Fluka (Stockholm, Sweden). Sodium acetate (puriss. ≥ 99.0 %, anhydrous), sodium bicarbonate (powder, ≥ 99.5 %), citric acid (anhydrous, ≥ 99.5 %), sodium citrate dihydrate (puriss. ≥ 99 %), glycine (puriss. ≥99 %), sodium L-tartrate dibasic dihydrate (ACS reagent, ≥ 99 %) sodium L-lactate (~98 %), and sodium pyruvate (SigmaUltra, ≥ 99 %) were purchased from Sigma Aldrich (Stockholm, Sweden).

The chemical composition of the two test media described in [91] is presented in Table 5. Samples from both pure and zeolite filled composites were cut to a dimension of 30x10 mm and placed into acid-cleaned (1 % HNO_3 for 24 h) glass vessels that were filled with 10 mL of either ALF or Gamble's solution, and thoroughly sealed with Parafilm. Subsequently, the

samples were placed in an incubator and stored under static and dark conditions at 37°C during 84 days. Samples were withdrawn from the solution on a weekly basis and analyzed.

Table 5. *Chemical composition of the artificial body fluids (g/l).*

Chemicals	ALF	Gamble
$MgCl_2$	0.050	0.095
NaCl	3.21	6.019
KCl	-	0.298
Na_2HPO_4	0.071	0.126
Na_2SO_4	0.039	0.063
$CaCl_2 \cdot 2H_2O$	0.128	0.368
$C_2H_3O_2Na$	-	0.574
$NaHCO_3$	-	2.604
$C_6H_5Na_3O_7 \cdot 2H_2O$	0.077	0.097
NaOH	6.00	-
$C_6H_8O_7$	20.8	-
H_2NCH_2COOH	0.059	-
$C_4H_4O_6Na_2 \cdot 2H_2O$	0.090	-
$C_3H_5NaO_3$	0.085	-
$C_3H_3O_3Na$	0.086	-
pH	4.5	7.4

3.3 CHARACTERIZATION TECHNIQUES

3.3.1 Scanning Electron Microscopy (SEM)

SEM micrographs from were taken from the surface of the samples with a Hitachi S-4800 Ultra-High Resolution Field Emission Scanning Electron Microscope (FE-SEM) (Hitachi High Technologies Europe GmBH, Krefeld, Germany) at different magnifications. SEM investigation was performed to study the possible surface alterations and degradation signs on the polymers and composites. The samples were first coated with gold/palladium. The thickness of the coating layer was approximately 10 nm.

3.3.2 Contact angle measurement

The contact angle measurements were performed on a CAM 200 instrument from KSV Instruments Ltd. (Helsinki, Finland) in order to monitor the change of the surface properties of the different samples. MilliQ grade water from a Synergy 185UV Ultrapure water system (18.2MΩcm, Millipore AB, Solna, Sweden) was used. The contact angle was measured on all exposed samples; the average value of three pieces cut from the same sample was calculated.

Five 3 µl droplets were analyzed on each piece, i.e. a total number of 15 droplets, and ten images were taken for each droplet at a speed of 100 frames/s.

3.3.3 Fourier Transform Infrared Spectroscopy (FTIR)

The aim of the FTIR analysis was the determination of chemical changes in the structure of the polymers and composites. For this purpose a Spectrum 2000 FTIR spectrometer from Perkin Elmer (Wellesley, MA, USA) equipped with a Golden Gate single-reflection accessory for Attenuated Total Reflection (ATR). Triplet of the samples were analysed, 16 scans per piece between 4000 cm^{-1} and 600 cm^{-1} were averaged at intervals of 1 cm^{-1} with a resolution of 4 cm^{-1}. All the spectra were normalized to 1.5 cm^{-1} and the results were averaged.

3.3.4 Matrix-Assisted Laser Desorption/Ionization Time-of-Flight Mass Spectromety (MALDI-TOF MS)

MALDI-TOF-MS measurements were performed on the silicone rubber samples in order to detect and identify any low molecular weight compounds that may have formed during the exposure of the silicone rubber samples and composes. For polyurethane it was not possible to conduct this technique, since polyurethane consists of a hard and a segment that need to be separated prior to the analysis. The separation of these segments can be done by selective degradation reactions [92, 93]. In the present case, the degradation products played a vital role in the understanding of the degradation phenomenon during *in-vitro* ageing, therefore the degradation products that form during the selective degradation reactions might influence the results.

A Bruker Ultraflex MALDI-TOF MS instrument with a SCOUT-MTP laser source from Bruker Daltonics (Bremen, Germany) was used to analyse the silicon rubber samples. The instrument was equipped with a nitrogen laser (337 nm), a grid less ion source and a reflector. The generated spectra were collected in the reflector, positive ion mode with an acceleration voltage of 25 kV and a reflector voltage of 26.3 kV. The mass range of the detector was set between m/z 900-2500, and the laser power was set slightly above the threshold. The samples analysed by the MALDI-TOF MS technique were spotted on a MTP 384 ground steel target plate (Bruker Daltonics, Bremen, Germany).

The following chemicals were used for MALDI sample preparation: sodium-trifluoroacetate (NaTFA) (purum, ≥ 98.0 %), heptane (puriss. p.a., ≥ 99.5 %) were purchased from Fluka (Stockholm, Sweden). Chloroform (≥99%), tetrahydrofurane (THF) (Chromasolv® Plus, for HPLC, ≥ 99.9 %), 2,5-dihydroxybenzoic acid (DHB) (puriss. p.a., matrix substance for MALDI-MS, > 99.0 %) were purchased from Sigma Aldrich (Stockholm, Sweden).

The low-molecular-weight silicone compounds were extracted from the surface of the samples by rinsing with 5 ml heptane. The extracts were placed in glass vials and the heptane was evaporated. Then the residue was dissolved in 1 ml chloroform [94]. DHB at a concentration of 10 g/l in THF was used as the matrix for the MALDI-TOF MS analyses. The analyte and the matrix solution were mixed in equal ratios, i.e. 10+10 µl, and doped with 4 µl NaTFA at 1 g/l in THF. Approximately 0.3 µl of the mixture was then spotted onto the target plate. Triplets were extracted and analyzed from each sample, and three spots were prepared on the target plate per extract. For the quantitative analyses the average values were calculated from the results of the triplets. The mass spectra were accumulated from 500 laser shots.

3.3.5 Hardness and tensile testing

Shore A and D hardness measurements were performed on unaged samples to monitor the effect of zeolite content on the hardness. The measurement was performed by a Zwick/Roell Shore Digital Hardness Tester (Zwick GmbH & Co. KG, Ulm, Germany) according to DIN 53505 and ASTM D 2240 standards.

The mechanical properties of the materials plays secondary role in this study, therefore tensile tests were carried to determine the influence of zeolite content on the mechanical properties of the composites. The test was performed on an Instron 5560 tensile tester (Instron, High Wycombe, United Kingdom) according to ISO 37 standard. Mini standard sized test specimens were cut out of both polyurethane and silicone rubber samples. A 10 kN load cell was applied to the instrument. The test temperature was 23 °C with 50 % of humidity. The specimens were conditioned under these conditions for at least 24 hours prior to the test. The tensile velocity was 10mm/min.

4 RESULTS AND DISCUSSION

4.1 ANTIMICROBIAL ZEOLITES

4.1.1 Maximum ion-exchange capacity

Figure 5 represents the ion adsorption isotherm of A zeolite. Silver ions were absorbed with the largest amount in the zeolite (~ 3.7 mmol/g). It is followed by zinc with absorption of 2.1 mmol/g and copper (1.4 mmol/g). On the isotherm curve of zinc and copper a plateau was observed, which characteristic indicates that the zeolite reached its maximum ion absorption capacity and become saturated. The amount of absorbed ions in the zeolite increases, as a function of the initial ion concentration in the solution up to 30 mmol/l. Between 50 and 100 mmol/l the amount of absorbed ions reached a maximum level and remained constant, which indicates that the zeolite became saturated.

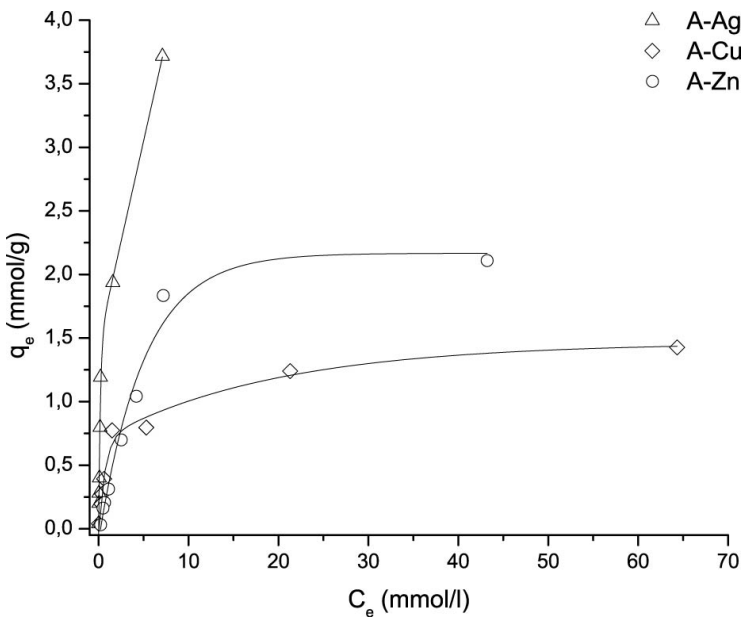

Figure 5. *Silver, copper and zinc ion adsorption isotherms of zeolite A.*

In order to confirm whether the zeolites became saturated between 50 and 100 mmol/l initial solution concentration, the determination of the maximum ion exchange capacity is necessary. This parameter can be determined from the linearized Langmuir ion absorption isotherms

(Fig. 6) or by equation (2). On the isotherm the gradient and the intersection values are used from the equation of each trendline to determine the maximum ion exchange capacity for the given ion in the zeolite.

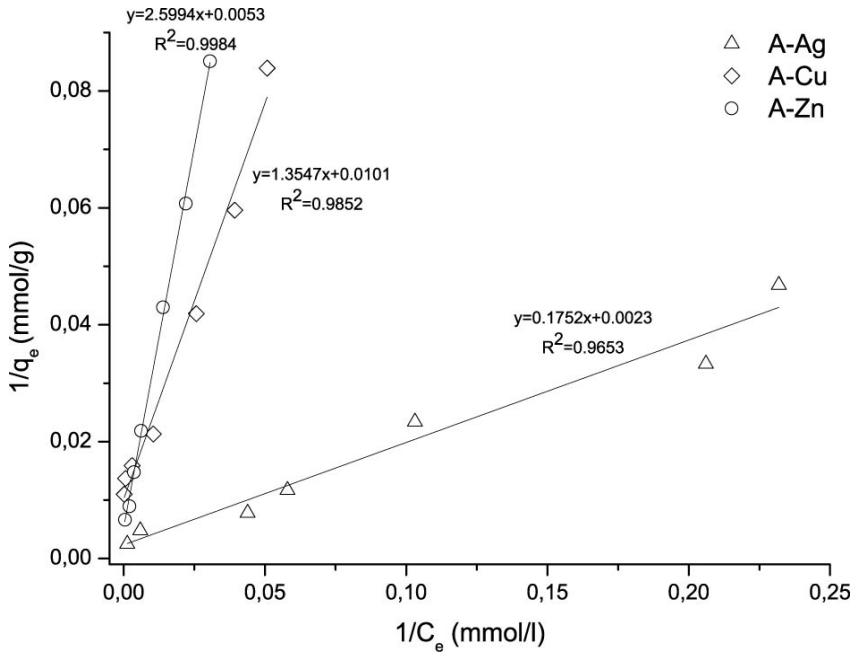

Figure 6. *Linearized Langmuir isotherm of silver, copper and zinc exchanged zeolite A.*

The theoretical maximum ion exchange capacity values and the measured amount of each ion at 100 mmol/l initial concentration are given in Table 6. The results show that the theoretical total ion absorption capacity was not reached in any of the samples at the initial ion concentration 100 mmol/l. In sample Ag, Cu the measured ion concentration is approximately 8-10 % lower, than the theoretical saturation point, which is acceptable. In contrast, mostly all absorption isotherms showed a nearly saturated level of the samples. This significant difference between the theoretical and measured values may be due to the equilibrium between the sodium and exchanging ion, since the zeolite was previously saturated with sodium in order to maximize the ion absorption capacity. Based on the results it seems that the ion adsorption isotherms are more likely to show only the absorption capacity and do not take into account that the solid phase may contain additional ions that can be exchanged. In the present case, due to a concentration gradient, sodium ions exchange with other ions until an equilibrium concentration is reached between the solid and liquid phase. The concentration of the sodium decreases in the solid phase as a function of the exchanger ion concentration in the solution. Due to the increasing concentration of the exchanger its activity coefficient

decreases which slows down the ion-exchange reaction and results in a decreased absorbed/remained ion concentration ratio. Therefore if an exchangeable ion is present in the solid phase, at higher initial ion concentrations the absorption isotherms show saturation characteristics and may give false data regarding to the saturation level.

Table 6. *Parameters of the linearized Langmuir isotherms and the comparison of maximum ion absorption (Q) capacity with the measured absorption at 100 mmol/l initial ion concentration.*

Sample	m	b	k_L (mg/l)	Q (mg/g)	Q at 100mmol/l
Ag	0,1752	0,0023	76,17	434,78	400,6
Cu	1,3547	0,0101	134,1287	99,0099	90,64
Zn	2,5994	0,0053	490,4528	188,6792	148,38

4.1.2 Single, binary and ternary ion-exchanged systems

After the theoretic determination of maximum ion adsorption capacities for the three metallic ions, the preparation of different multi ion containing systems was performed. The aim for single ion-exchanged system was to reach and confirm the theoretical saturation level of the zeolites, which was determined by the linearized Langmuir isotherms. The main objective of binary and ternary ion-exchanged systems was to determine the concentration distribution of the ions in the system if the initial concentration of each ion is equal in the ion-exchange solution. The results are presented in table 7.

Table 7. *Calculated and measured maximum silver, copper and zinc ion concentrations in A zeolite.*

Sample	Ions (m/m%)		
	Ag	Cu	Zn
Ag	44,47 (43,48)		
Cu		9,25 (9,9)	
Zn			18,38 (18,68)
Ag-Cu	34,71	4,87	
Ag-Zn	40,8		3,37
Cu-Zn		8,43	7,39
Ag-Cu-Zn	35,7	4,85	1,58

*values in brackets are the theoretically calculated maximum ion adsorption values

In the single ion-exchanged system the measured maximum absorbable ion concentrations confirmed the accuracy of the theoretically determined maximum ion exchange capacity. This means that even though the characteristics of the adsorption isotherms may indicate the saturation level incorrectly, the linearized Langmuir isotherms give accurate results on the maximum ion exchange capacity.

As it can be obtained from both the adsorption isotherms and the EDX results, the silver cation was the most preferable by the zeolite. It is known that zeolite structures have selectivity against the different cations. This is influenced by the ionic radius, the activity of the ions and by the valences in the crystal structure. The experiments showed that the ion selectivity for zeolite A was Cu < Zn < Ag. Although the atomic radius of Ag (1.65 Å), Cu (1.45 Å) and Zn (1.42 Å) is similar [95], the ionic radius of Ag (1.29 Å) ions is approximately 1.8 times bigger than Cu (0.71 Å) and Zn (0.74 Å) [96]. In the aqueous solutions hydration of the ions takes place where ions with smaller diameter have larger specific surface area, therefore become more hydrated. Due to hydration a hydration sphere can be determined around the ion, which is the summed diameter of the ion and the surrounding oxygen atoms. Since Ag has a smaller specific surface area the hydrated ionic radii will be ~2.5 Å while for Zn and Cu this radius was previously determined to be ~6.8 Å [97]. This size increase results in a decreased activity coefficient, which is one of the main reasons for the moderate or poor absorption of Cu and Zn ions in the different binary and ternary zeolite systems. The ionic strength (μ) (Eq. 3) and activity coefficients (γ) (Eq 4) of the solutions were calculated according to the following equation, and are presented in Table 3.

$$\mu = \frac{1}{2}\sum_i z_i^2 C_i, \tag{3}$$

$$\log\gamma_i = \frac{-0.509 z_i^2 \sqrt{\mu}}{1+(3.29\alpha_i\sqrt{\mu})}, \tag{4}$$

where z represents the charge of the ion, C is the concentration and α is the hydrated ionic radius.

In binary and ternary systems the amount of silver ions decreased compared to single ion-exchanged systems but still zeolites absorbed them with the highest concentration. In the two component Ag-Cu and Ag-Zn systems the amount of Cu and Zn ions were similar, slightly more Cu was exchanged in the zeolite than zinc. However in the Zn-Cu and three component systems the amount of Zn was significantly lower than Cu. Based on the literature there is no significant difference in the ionic and hydrated ionic radii for Cu and Zn. Due to the similar size both ions may be bonded at similar sites of the crystal, therefore they can occupy each other´s place that indicates the decreased amount of both ions in binary and ternary systems.

The adsorbed amount of silver also decreased in multi-component systems, which is indicated due to Cu and Zn may occupy and block crystal sites where Ag bonds. Furthermore since EDX only measures the composition of an analyte in atomic or weight percent, it is also probable that in binary and ternary systems the amount of neither atom is decreased and the observed decrease in weight percent is only apparent due to the difference in the atomic weights of the different elements.

Table 8. *The activity coefficients and ionic strength of the exchange solutions.*

Ionic solutions	γ			μ (mol·dm^{-3})
	Ag	Cu	Zn	
Ag	0.745			0.1
Cu		0.291		0.3
Zn			0.291	0.3
Ag-Cu	0.614		0.267	0.4
Ag-Zn	0.614	0.267		0.4
Zn-Cu		0.238	0.238	0.6
Ag-Zn-Cu	0.559	0.228	0.228	0.7

4.1.3 Ion release of single, binary and ternary ion-exchanged systems

The antimicrobial activity of the zeolite is based on the amount of antimicrobial ions that are re-exchanged –or released- from the structure during the use of the material. In the single ion systems the release of the ions depends on the exchanging cation, the ionic strength of the solution and the selectivity of the zeolite for the ingoing and out-coming ions. If the zeolite prefers the outgoing ion the ion release and exchange rate will be minimal. This is due to the ionic forces that keep the ions in the structure and results a decreased activity and mobility of the ion. If the system has better selectivity against the ions in the environment the ions in the zeolite can be easily exchanged. In multi-ionic systems this phenomenon is more complex. In binary or ternary ionic systems the ions in the structure have different selectivity and during a re-exchange reaction these ions may compete with each other, which influences the release rate. Based on the location of the ions in the structure, ions that are more preferred by the zeolite can block the way of other ions that are less preferred. Due to this, both ions may stick in the system and no or minimal re-exchange could be observed. Figure 7 represents the released concentration of Ag, Cu and Zn ions from the different multi-ionic systems as a function of the initial concentration of sodium chloride solution.

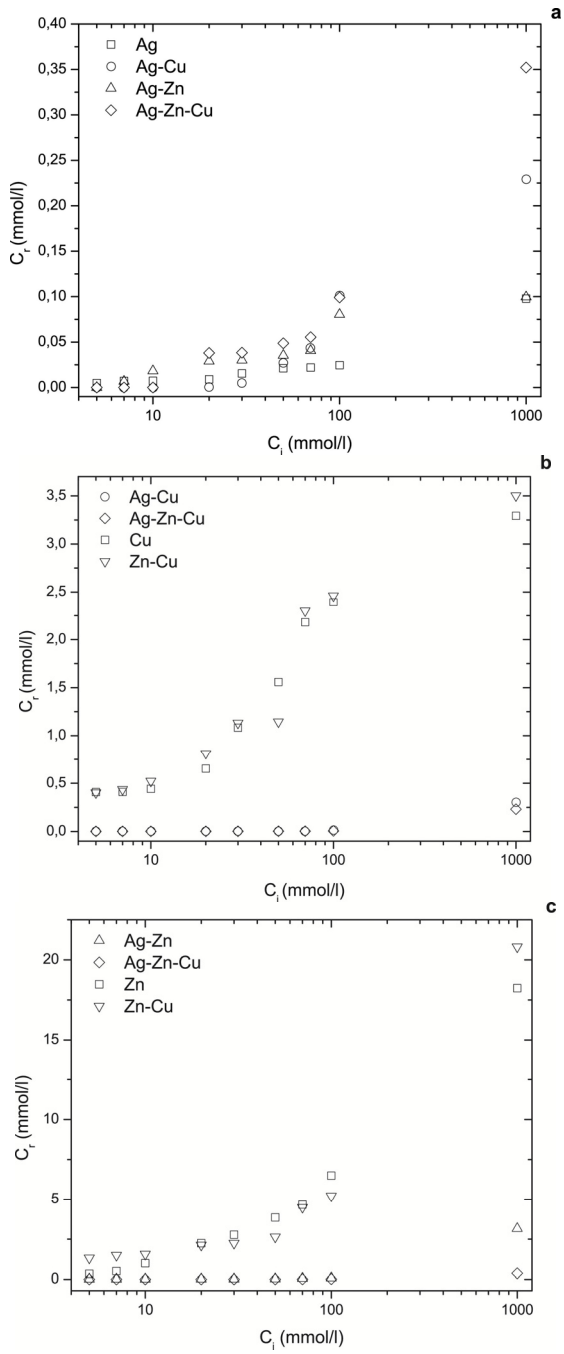

Figure 7. *The release of silver (a), copper (b) and zinc (c) ions as a function of initial sodium concentration.*

In all the samples Ag was the ion that was released with the least amount from the structure. The concentration of the out-coming silver ions increases as a function of the concentration of NaCl solution, however the release is not significant. The maximum released concentration of silver was found to be 0.35 mmol/l while the total silver concentration that may be released into the solution was 96.2 mmol/l. It was again confirmed at the sodium exchange to silver, that silver is highly preferred by zeolites. The high selectivity of silver may be one of the reasons for the low amount of silver release. Another reason could be the reduction of silver ions to silver-oxide, which may have occurred during the sample preparation at drying stage. It is known that silver ions in solutions are very sensitive to environmental impacts i.e. light, heat etc. therefore it is probable that ions are reduced to oxide during the drying of the samples.

Copper and zinc ions are less sensitive and show relatively high stability in solutions or solid structures. For copper ion the lowest concentration was released from the zeolite in case of those binary and ternary systems (Ag-Cu, Ag-Zn-Cu) where silver was also present. The minimal copper release of these systems therefore can be influenced by the silver ion. Most probably copper is located in the crystal structure somewhere below silver ions, therefore silver blocks the copper´s way out from the structure. The silver and copper release of these samples is in accord. For samples that contain only copper or zinc-copper ions, the released amount of copper increased compared to the samples where silver was present, however, this quantity seemed to be relatively low (~3 mmol/l). These results confirm that both copper and silver are preferred by the zeolite and are less likely to exchange with Na ions.

Table 9 summarizes the initially exchanged amount of sodium and re-exchanged Ag, Cu and Zn ions in weight percentage. During the initial ion exchange, 100 % of the sodium was exchanged by the three ions in the different single, binary and ternary systems. The re-exchange results show that minimal amount (0.1-0.45 %) of silver was released from the different zeolite systems. Binary ion exchanged samples containing silver and copper and ternary ion exchanged systems released only 1.29-1.68 % of the total copper amount from the structure which confirms that the presence of silver has a great influence on the release of copper. In contrast, samples that did not contain any silver ions released approximately 10 times more copper. As it is obvious from the ion-release graphs the zinc was released with the greatest amount from the structure. The release of this ion doesn't seem to be influenced by the silver. The minimum amount of zinc was released from the ternary ion exchanged system and the highest amount was exchanged from the binary, zinc-copper zeolite. These results confirm that copper and zinc ions due to their similar activity are competing with each other during both the absorption and release. Therefore the presence of these two ions in the system influences each others´ ion exchange properties.

Table 9. *The percentage of exchanged ions during the ion exchange and re-exchange reactions for zeolite A.*

Sample	% Exchanged	Re-exchanged %		
	Na	Ag	Cu	Zn
Ag	100	0.1		
Cu	100		9.69	
Zn	100			27.81
Ag-Cu	100	0.31	1.68	
Ag-Zn	100	0.11		26.27
Zn-Cu	100		11.32	78.94
Ag-Zn-Cu	100	0.45	1.29	6.65

4.1.4 Theoretical distribution of ions in the crystal structure

Based on the previously discussed ion exchange and release results the estimated ion distribution in the structure of zeolite A can be determined. After the literature data was compared with the composition (Table 10) and ion release of the samples, the suggested theoretical distribution of ions in the structure of the zeolite was constructed. In table 5 the experimental data is compared with the theoretical composition (in brackets) of the zeolite.

The distribution of silver and sodium ions in the structure is quite similar and the experimental values are in a good correlation with the theoretical data.(Fig. 8a-b). The main difference between these two systems is that in silver exchanged zeolite three additional silver ions are adsorbed, which are located at the corner of the unit cell [98, 99]. Besides, copper (Fig. 8c) and zinc (Fig. 8d) ions are located in the sodalite cages similarly to the sodium and silver [100]. The ion exchange in binary and ternary exchanged systems occurs in the sodalite cage regions. Based on the released amount of the ions in silver-copper system (Fig. 8e) the silver ion should be located at the external site of the sodalite cage and blocking the way of copper ions for release. In silver-zinc system the distribution is a bit more complex. In single zinc exchanged zeolite two zinc ions occupy one sodalite cage (Fig. 8d) while one sodium, silver or copper is trapped at the same location (Fig. 8a-c). In binary zinc-silver system it seems from the release rates that within the sodalite cage one silver ion is surrounded by two zinc ions (Fig. 8f). Therefore zinc which is located on the outer area exchanges easily with the ions from the solution and the way of the second zinc ion is blocked by the silver ion, which is less likely to re-exchange with sodium. In zinc-copper zeolite the amount of zinc that is adsorbed in the zeolite is half compared to single ionic system. This may due to the presence

of copper, which has same almost the same size and activity as the zinc and is competing with it.

Table 10. *Theoretical composition of the built crystal structures compared to the measurement data for zeolite A.*

Sample	O	Al	Si	Cu	Zn	Ag	Na
	wt %						
Na	41.94 (45.05)	20.59 (18.99)	21.29 (19.77)				16.18 (16.19)
Ag	29.28 (28.2)	13.3 (11.89)	13.54 (12.38)			43.88 (47.53)	
Cu	54.29 (51.2)	17.78 (17.27)	18.58 (17.96)	9.35 (13.56)			
Zn	46.3 (47.69)	17.01 (16.08)	18.07 (16.74)		18.62 (19.49)		
Ag-Cu	34.06 (30.29)	12.63 (10.22)	13.72 (10.63)	4.87 (8.02)		34.73 (40.84)	
Ag-Zn	32.44 (29.02)	11.47 (9.79)	11.91 (10.19)		3.3711.86	40.8 (39.14)	
Zn-Cu	50.67 (47.82)	15.18 (16.13)	16.78 (16.79)	8.51 (9.5)	8.87 (9.77)		
Ag-Zn-Cu	32.91 (29.63)	14.13 (13)	10.82 (12.49)	4.85 (9.81)	1.58 (10.09)	35.7 (24.97)	

*values in brackets are the theoretically calculated data

The result is, that the same amount of copper can be absorbed in this binary system and due to the copper occupying the place of one of the zinc ions only one can be further absorbed. The release results showed that copper is absorbed first then the remaining outer spaces are filled with zinc ions (Fig 8g). In ternary system the release of each ion was poor. It was observed in the zeolite that silver can be the responsible for the poor release of the other ions in multi-ionic systems, therefore in a ternary system the most probable location of the silver ion is the outer space of the sodalite cage and followed by zinc and copper (Fig. 8h).

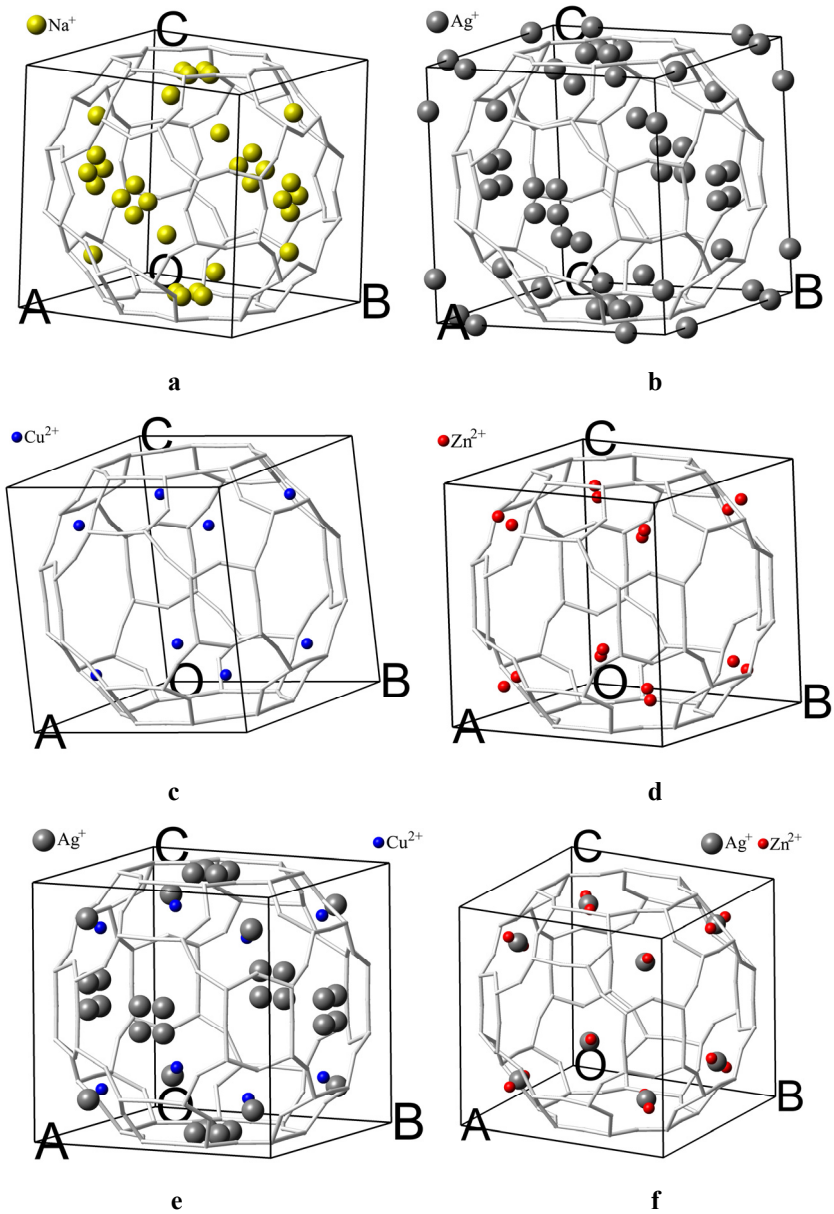
Na+
C
A
O
B
a
Ag+
C
A
O
B
b
Cu2+
C
A
O
B
c
Zn2+
C
A
O
B
d
Ag+
Cu2+
C
A
O
B
e
Ag+
Zn2+
C
A
O
B
f

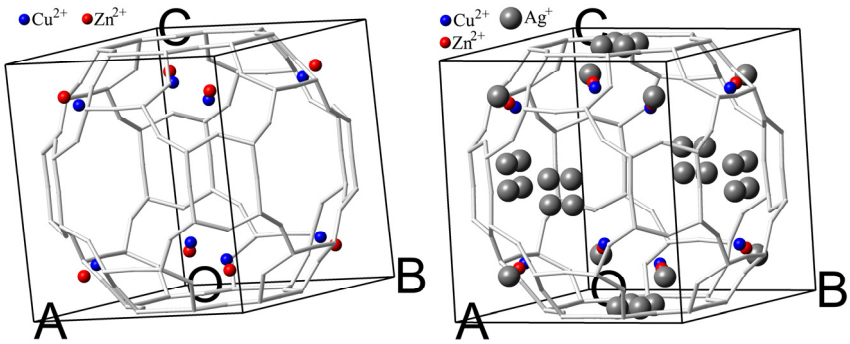

g **h**

Figure 8. *Theoretical distribution of ions in the structure of zeolite A. (a) sodium-, (b) silver-, (c) copper-, (d) zinc-, (e) silver-copper-, (f) silver-zinc-, (g) zinc-copper-,(h) silver-copper-zinc exchanged zeolite A.*

4.1.5 Antimicrobial activity

Recent studies have presented that silver-zeolite, copper and zinc shows efficiency against microbes. This effect of binary and ternary ion exchanged system has not been investigated yet. This part of the study is dedicated to fill this gap in the literature and to determine whether the multi-ionic zeolite systems give an increased antimicrobial efficiency or not. Table 6 represents the MIC of the zeolite samples against *Candida tropicalis*, *Pseudomonas aeruginosa* and methicillin-resistant *Staphilococcus aureus* (MRSA).

Table 11. *Minimum inhibitory concentrations of ion exchanged A (ppm).*

Sample/Strain	*Candida tropicalis*	MRSA	*Pseudomonas aeruginosa*
REF	>1024	>1024	>1024
Ag	2	512	128
Cu	2	>1024	1024
Zn	512	>1024	1024
Ag-Cu	256	1024	256
Ag-Zn	64	512	512
Zn-Cu	512	512	1024
Ag-Zn-Cu	512	512	512

The reference zeolite sample that did not contain any ions did not show any antimicrobial efficiency against any of the microorganisms, which was expected. For *Candida tropicalis* the MIC of Ag, Cu and Ag-Zn samples were superior compared to the other samples. Zn, Zn-Cu and Ag-Zn-Cu zeolites were equally efficient against this strain. In case of MRSA the MIC

value of all zeolite samples was higher compared to the other strains. Besides the reference zeolite Cu and Zn samples didn´t express efficiency against this strain. In addition, Ag and the other binary and ternary exchanged systems, except for Ag-Cu, had the same MIC value for MRSA. Ag exchanged zeolite was superior against *Pseudomonas aeruginosa* compared to the other samples. The performance of Ag-Cu was adequate; furthermore, the binary Ag-Zn and the ternary ion exchanged sample had the same MIC value against this strain (512 ppm), which is an acceptable antimicrobial efficiency. The rest of the samples showed minimal antimicrobial performance. Besides the determination of MIC, agar diffusion test was also performed on the zeolite samples. These results are presented in Table 12.

Each microorganism formed inhibition zones around most of the samples. No inhibition zone was observed around the reference sample in case of all three microorganisms and around Cu, Zn in case of MRSA. For this strain Ag inhibited the cell growth in the highest range. The inhibition range of binary ion exchanged zeolites was similar (10-12 mm) while MRSA cells started to grow in the smallest distance from the ternary ion exchanged sample (8 mm). In case of *Candida tropicalis* the size of the inhibition zone of the different samples was similar. However the biggest zone was measured around the Ag and Zn-Cu samples. This strain formed an inhibition zone with a diameter of 8 mm around the other samples, except for Ag-Zn-Cu where this value was lower (6 mm). The inhibition zone for *Pseudomonas aeruginosa* was determined to be the highest for Ag, Zn-Cu and Ag-Cu samples. The Cu, Zn and Ag-Zn-Cu showed similar efficiency in the inhibition range (8-9 mm) and Ag-Zn showed a bit better performance (12 mm).

Table 12. *The results of agar disc diffusion test (mm).*

Sample/Strain	*Candida tropicalis*	MRSA	*Pseudomonas aeruginosa*
REF	0	0	0
Ag	10	20	20
Cu	8	0	8
Zn	8	0	9
Ag-Cu	8	10	20
Ag-Zn	8	10	12
Zn-Cu	10	12	20
Ag-Zn-Cu	6	8	8

Based on the MIC and agar diffusion results it was seen that these two different antimicrobial properties are highly strain and ion dependant. In addition these results correlates well with the ion release results. For multi ionic systems the ion distribution in the zeolite structure and the release order of the different ions seemed to influence the antimicrobial efficiency. The different ions can block the absorption of the other ions within the microorganism cell. This

results in a lower antimicrobial activity of the multi ionic systems. It is clearly visible in case of zinc. In all of the zinc containing samples the zinc ions were released with the highest amount. Since this ion has a smaller size than the silver, the absorption of the zinc is faster and easier for the microorganisms. This indicates that the microorganism absorbed a higher amount of zinc during the antimicrobial test than silver. After the zinc absorption the absorption of other ions by the cell is blocked. In case of Ag-Cu samples the same mechanism could be the responsible for the decreased antimicrobial efficiency since Cu has a smaller ion size then the Ag. For Zn-Cu and Ag-Zn-Cu samples this process is more complex since the size of both ions is approximately the same. Here the location of the ions in the zeolite structure plays a vital role. Zinc is located on the outer part of the crystal and is followed by the copper. Therefore first zinc ions are released and their absorption by the microorganism starts immediately. When the subsequent release of copper occurs, a lower concentration of this ion will be absorbed from the solution by the microorganism compared to the single ionic Cu zeolite.

It can be concluded that the antimicrobial efficiency of Ag seemed superior to the other samples during the two tests. Besides, Ag-Zn and Zn-Cu samples may also have a potential.

4.2 Influence of Zeolite Content on the Properties of Antimicrobial Composites

4.2.1 Dispersion and surface properties

One major challenge in fabrication of composite materials is to obtain a homogeneous dispersion of the filler material in the matrix. The main advantage of zeolite particles compared to metals is that they are less likely to form agglomerates in the polymer during the mixing therefore homogeneous dispersion can be obtained. The zeolite distribution in the polyurethane and the silicone rubber composites was investigated with SEM (Figure 1) after the mixing process.

It could be determined from the SEM micrographs (Fig. 9) that the zeolite particles were evenly distributed in each composite. In polyurethanes the grain size in the structure was approximately 2-3 μm that matches the average size of the zeolite particles. This indicates that no agglomeration took place in the polyurethane structures. In silicone rubber a minor size increase of the zeolite was observed, which was determined to be 3-5 μm. This is due to the small degree of agglomeration of zeolite in the silicone rubber. Apart from the size increase the grain distribution in the silicone rubber was still homogenous.

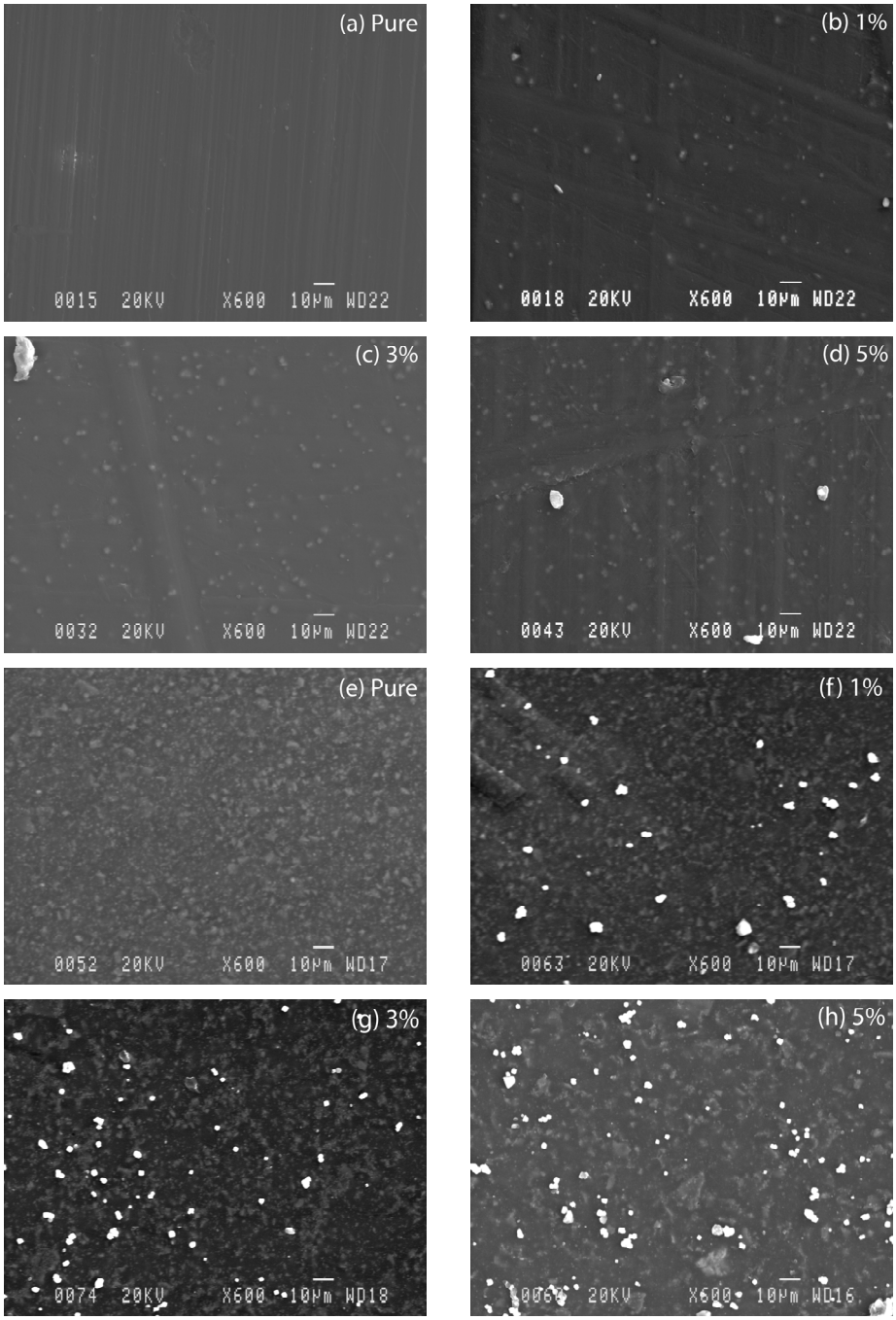

Figure 9. *SEM micrographs of zeolite loaded TPU (a-d) and silicone rubber (e-h) composites after mixing.*

The wettability of the composite materials was investigated since this surface characteristic plays a vital role in biofilm adhesion. The results of the contact angle measurements are presented in Figure 10.

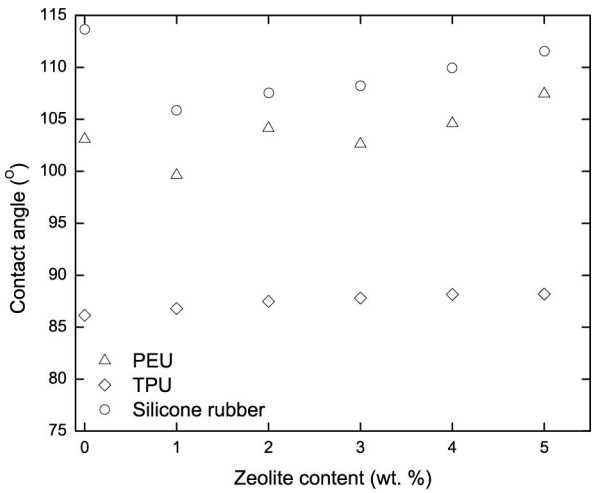

Figure 10. *The contact angle change of polyurethane and silicone rubber composites as a function of zeolite content.*

In general the contact angle showed a slight increase with the increasing the zeolite concentration in each composite. This indicates that zeolite content has influence on the wettability of the polymers. It was expected that due to the higher zeolite content the wetabbility would decrease, since it is a highly hygroscopic material. However, due to processing and sample preparation the zeolite particles that are encapsulated on the surface of the composites result change in the surface pattern of the composites that increased the hydrophobicity.

4.2.2 Mechanical properties

The results of the hardness measurements of the composites are presented in Figure 11. Slight increase was observed in the hardness of the composites as a function of zeolite content. This was expected, since zeolite is known to be a harder material than polymers.

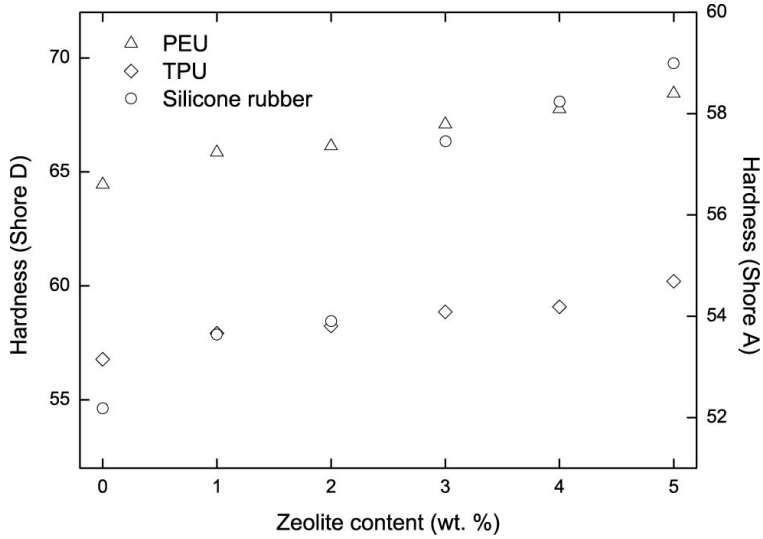

Figure 11. *The hardness increase of the composites as a function of zeolite content.*

*Polyurethanes: Shore D; Silicone rubber: Shore A

Despite of the hardness results, tensile test measurements showed significant changes in the physical properties of the materials. Figure 12 represents the tensile strength and Young's modulus of the composites and Figure 13 represents the elongation as a function of zeolite content.

The tensile strength and the elongation decreased significantly in case of each composite by the increasing zeolite content. At 5% zeolite content the tensile strength of polyurethane composites decreased by ~25% compared to the pure samples while silicone rubber lost ~40% of its tensile strength. Similar decrease was observed in the elongation of the composites, ~15-20% decrease was determined for polyurethane composites and ~50% for the silicone rubber. Smaller change was observed in the Young´s modulus of the samples. For both polyurethane composites the modulus decreased with 11-13%. The elastic modulus of silicone rubber increased as a function of zeolite content, at 5% it was determined to be 30% more than the initial value. These results indicate that the zeolite has significant effect on the mechanical properties, however due to the aim of this study and the future application of these composites, these characteristics play only secondary role.

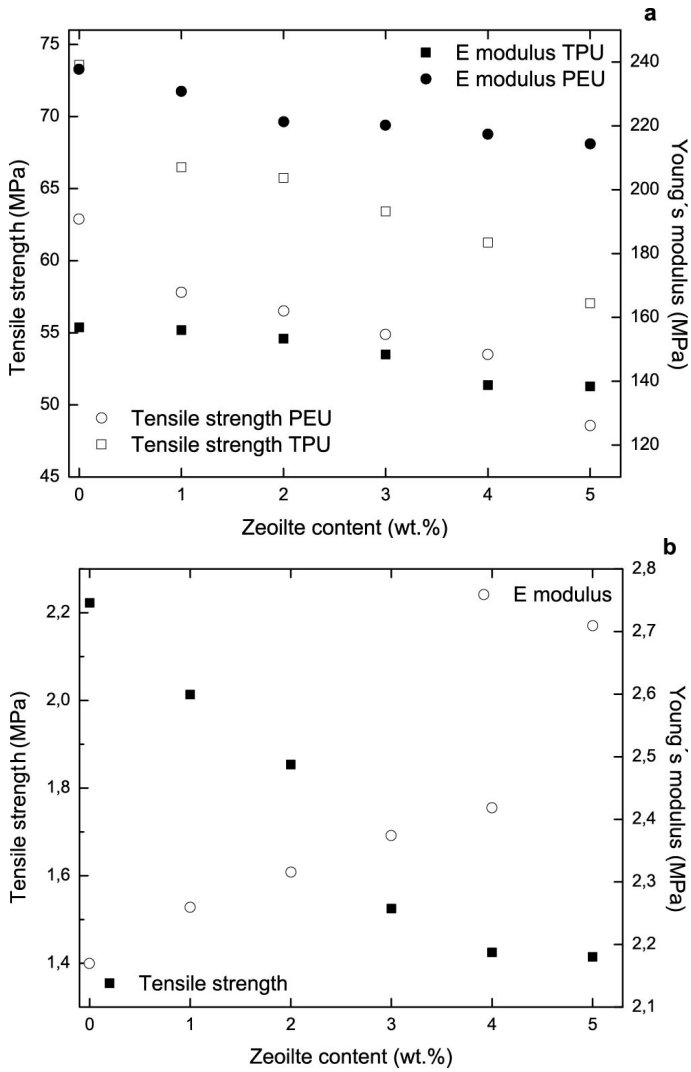

Figure 12. *Tensile test results of zeolite filled polyurethane (a) and silicone (b) composites.*

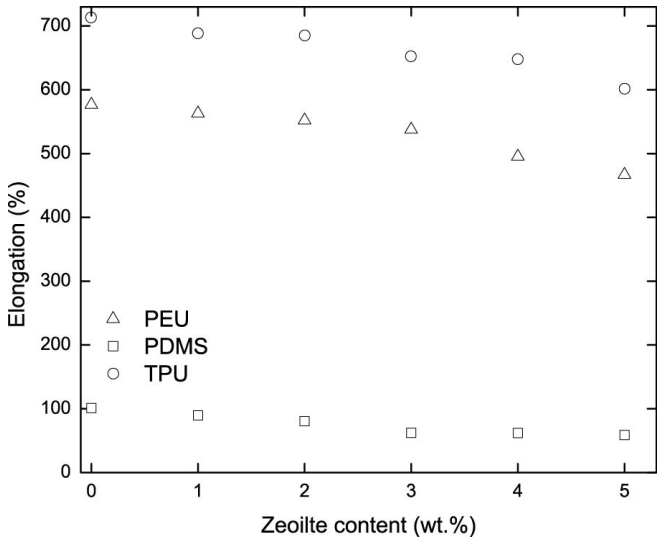

Figure 13. *Elongation of the composites as a function of zeolite content.*

4.2.3 Antimicrobial activity

Figure 14a shows the results of the antimicrobial test of zeolite filled TPU and silicone rubber composites as a function of zeolite content. Pure TPU did not show any antimicrobial effect as the number of viable cells increased on the surface after 24 hrs exposure compared to the initial cell concentration ($8 \cdot 10^6$ CFU/ml). The increase of the zeolite content resulted in improved antimicrobial effect. It was expected, since the concentration of silver increases with the increasing zeolite content. The reduction in viable cells was found to be the highest against *Candida tropicalis* for TPU composites. In addition, significant efficiency was observed against MRSA and *Pseudomonas aeruginosa* as well. In contrast to pure TPU, pure silicone rubber showed antimicrobial effect against all three species (Fig. 14a). Silicone composites were found to be the most efficient against *Pseudomonas aeruginosa* and showed slight antimicrobial effect against MRSA. The obtained results showed clearly that the antimicrobial effect of the different composites is material, strain and zeolite content dependant. The antimicrobial results of different ion-filled zeolite-PEU composites are presented on Figure 14b.

It was observed that pure PEU had no antimicrobial effect, as a result all of the microorganisms started to grow intensively on the surface. After 24 hours exposure the number of viable cells increased approximately one order of magnitude for MRSA and *Candida tropicalis* while for *Pseudomonas aeruginosa* this value became two times higher than the initial cell concentration ($5 \text{x} 10^5$ CFU/ml).

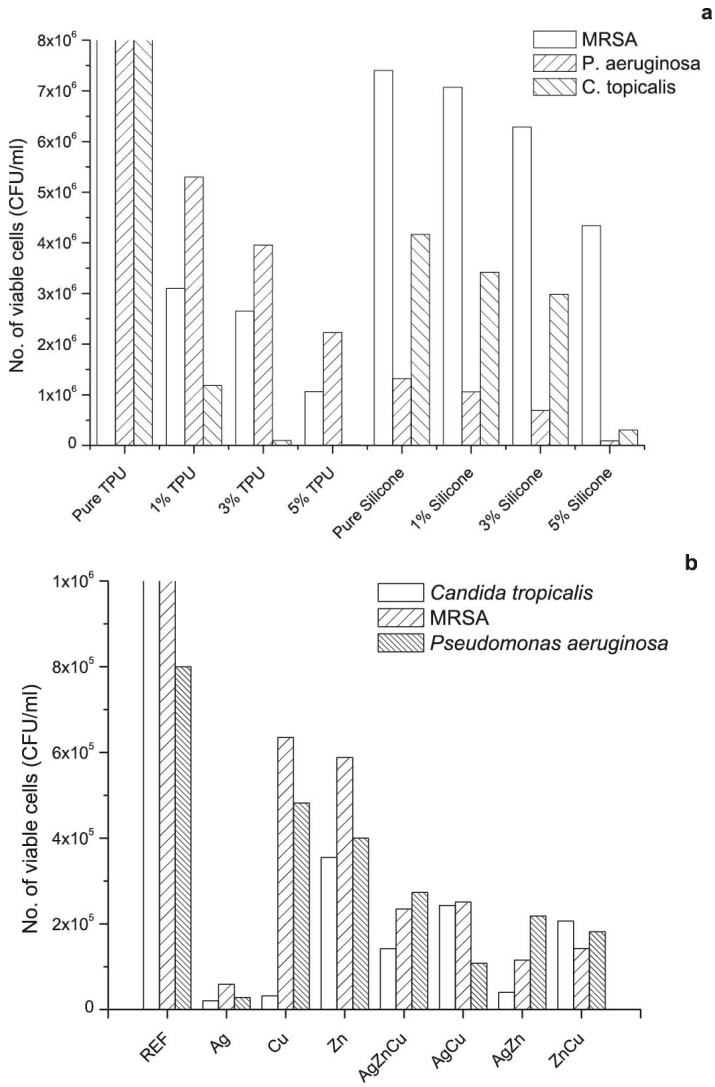

Figure 14. *The antimicrobial efficiency of the composites with increasing zeolite content (a) and constant zeolite content with different ions (b).*

In addition the number of viable cells for MRSA slightly increased on the surface of the composites that contained only copper or zinc zeolite as well. In contrast these samples showed growth inhibition effect against *Ps. aeruginosa* and *C. trop*. Both copper and zinc containing samples slightly decreased the number of viable cells for *Ps. aeruginosa*, and copper decreased the number of *Candida tropicalis* cells significantly as well. Binary and ternary ionic zeolite samples showed similar antimicrobial activity against all three microorganisms. However silver containing samples were superior to all of the other samples.

Based on this it can be assumed that in multi-ionic systems the silver ion could be responsible for the increased antimicrobial activity compared to single ionic copper and zinc zeolite. Although one by one these two ions did not express significant antimicrobial activity, the binary zinc-copper system decreased the number of viable cells with the same intensity as the silver containing multi-ionic systems. This increased efficiency could be due to joint activity of copper and zinc. It can be assumed that these ions initiate different toxic mechanism within the cell therefore the duplex system can be more harmful for the cells than single ones.

4.3 *IN VIVO* DEGRADATION OF SILICONE RUBBER

First of all SEM was used to study the surface structure of reference and *in vivo* used tracheostomy tubes. Figure 15a represents the SEM micrograph of the surface of the reference material, which has never been exposed to human body. The typical "worm-like" pattern of the ´Superslick coating´ was observed. After 1-month exposure the surface of the samples (Figs. 15b, c and d) were similar to the reference material (Fig. 15a). No significant surface changes were observed, which indicates that during the first month either no degradation took place or the influence of it cannot be detected. After three months exposure (Figs. 15e, f, and g), the surface of area 1, 2 and 3 were significantly altered compared to the reference sample. On the topography of area 1 (Fig. 15e), a network of cracks had formed on the surface. Since the shape of the cracks was irregular, it seems likely that this surface alteration is not due to mechanical stress. On area 2 (Fig. 15f), the pattern of the ´Superslick´ coating smoothened and became unrecognizable compared that indicates the wear of the coating. The surface of area 3 (Fig. 15g) is similar to area 2 (Fig 15f), and it seems that the coating almost vanished from the surface. Similar surface changes were also observed after six months exposure. On area 1 (Fig. 15h) and 2 (Fig. 15i) a parts of a biofilm or other biological media was occasionally detected. In addition the ´Superslick´ coating has completely disappeared from both locations, which indicates higher degree of degradation. On area 3, (Fig. 15j) the coating pattern smoothened, and hardly recognizable.

These results showed that during the in vivo exposure, surface degradation of the tracheostomy tubes initiated and a high degree of deterioration took place between 3 and 6 months that may shorten the lifetime of the material.

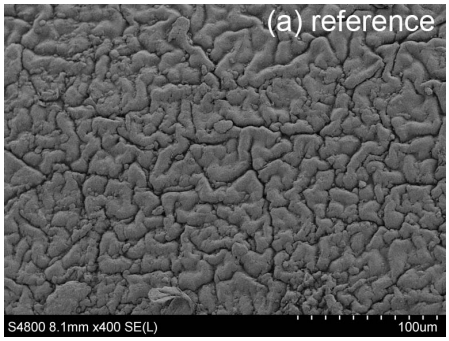
(a) reference
S4800 8.1mm x400 SE(L)
100um

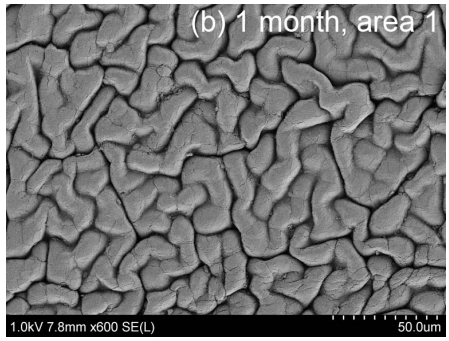
(b) 1 month, area 1
1.0kV 7.8mm x600 SE(L)
50.0um

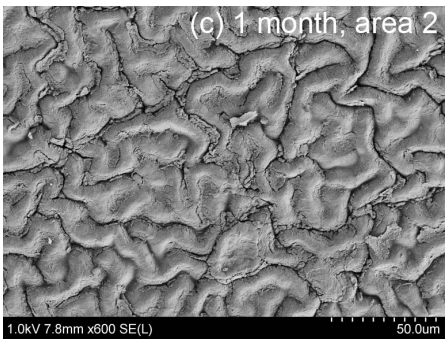
(c) 1 month, area 2
1.0kV 7.8mm x600 SE(L)
50.0um

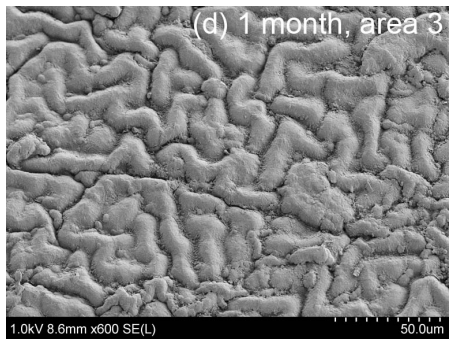
(d) 1 month, area 3
1.0kV 8.6mm x600 SE(L)
50.0um

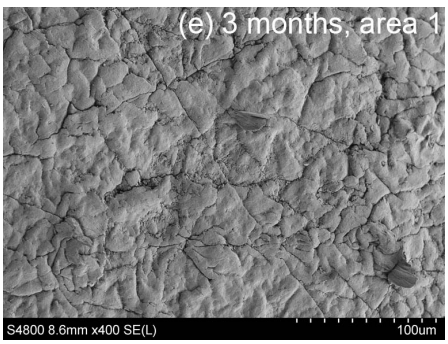
(e) 3 months, area 1
S4800 8.6mm x400 SE(L)
100um

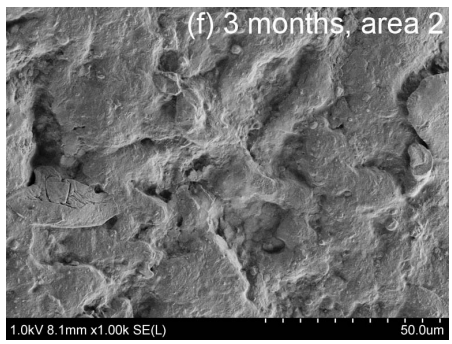
(f) 3 months, area 2
1.0kV 8.1mm x1.00k SE(L)
50.0um

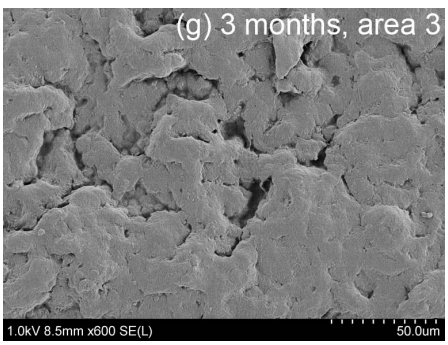
(g) 3 months, area 3
1.0kV 8.5mm x600 SE(L)
50.0um

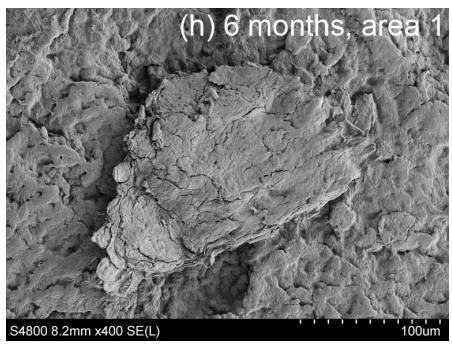
(h) 6 months, area 1
S4800 8.2mm x400 SE(L)
100um

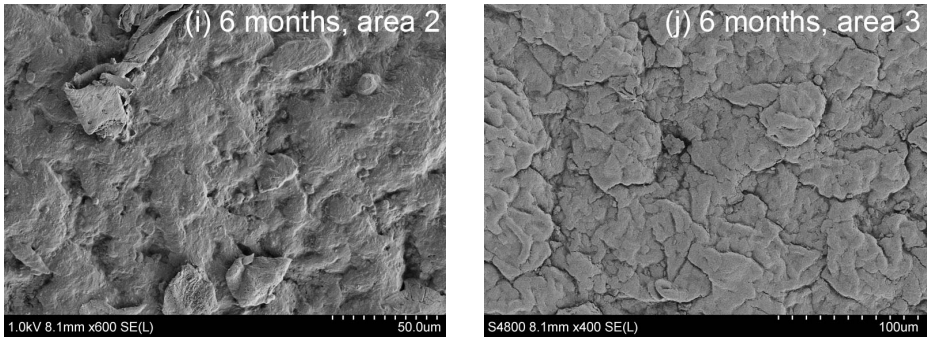

Figure 15. *SEM micrographs from the surface of silicone rubber (a), unexposed sample; (b-d), area 1,2 and 3 of one-month in vivo used sample; (e-g), area 1,2 and 3 of three-month in vivo used sample; (h-j), area 1,2 and 3 of six-month in vivo used sample.*

Contact angle measurements were performed to detect changes in surface properties based on the SEM investigations. Table 13 shows the measured contact angle values at area 1, 2, and 3 on each tube at various exposure times. Figure 16 shows the average values from all patients as a function of time with respect to each area. The standard deviation of the contact angle values varied between 1.4 º and 9 º.

Table 13. *The contact angle change of the different tracheostomy tube samples according to the sampling area and exposure time.*

Contact angle (°)				
Sample	Area 1	Area 2	Area 3	Exposure time (month)
SIL-reference	115	115	115	0
SIL-205	118	113	101	1
SIL-206	116	111	114	3
SIL-208	111	107	108	6
SIL-209	110	110	109	1
SIL-210	115	113	111	3
SIL-212	122	118	122	6
SIL-213	123	111	112	1
SIL-214	119	120	118	3
SIL-216	115	114	114	6
SIL-217	117	122	120	1
SIL-218	115	109	116	3
SIL-220	107	105	107	6
SIL-221	124	114	92	1
SIL-222	116	112	113	3
SIL-224	114	112	115	6

No significant trend was observed in the change of contact angle. In some cases, e.g. sample SIL-212 area 1, the measured contact angle was higher than for the reference tube, while in other cases the contact angle was lower compared to the reference. A possible explanation to the increase phenomenon could be that the biofilm was not completely removed from the surface during the cleaning. It is known that the surface of biofilms is hydrophobic in order to protect the contained microorganisms from the surrounding environment [101, 102].

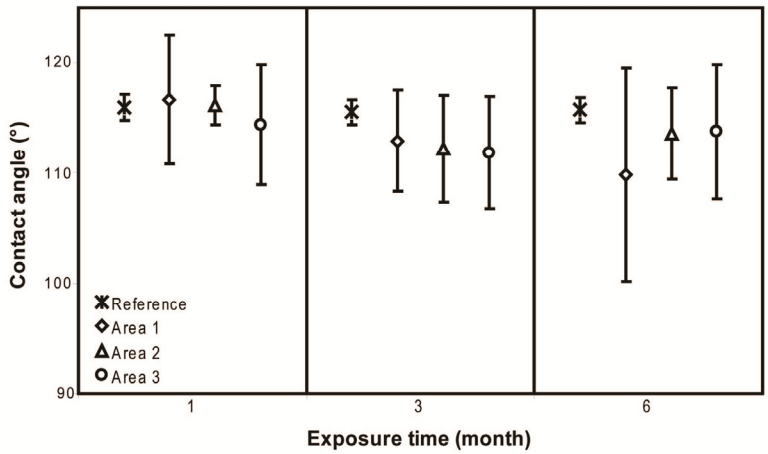

Figure 16. *The contact angle measurement results of the reference sample and in vivo used samples (according to sampling area 1, 2 and 3) as a function of exposure time.*

Several parameters, some of which may also be due to post *in vivo* treatment, e.g. cleaning, of the tubes, may influence the results. It was expected that the surface hydrophobicity would decrease due to wear of the hydrophobic ´Superslick´ coating and/or changes in the chemical structure of the polymer molecules at the tube surface. An explanation for the increase in contact angle could be the "self-healing" phenomenon that has been observed in silicone rubbers. It has been shown that diffusion of hydrophobic linear low-molecular-weight silicon molecules from the bulk to the surface of the plastic could increase the contact angle [103-107].

The slight decrease of the contact angle could be a result of de-crosslinking and chain scissions on the surface. Degradation of silicone rubbers in a strongly acidic environment [108], which is present inside the human body, predominantly occurs through hydrolysis. Thus, relatively hydrophilic hydroxyl-terminated compounds are formed which are known to be linear or cyclic low molecular weight compounds. These molecules are hydrophilic and therefore the presence of these molecules may be another reason for the decreased contact angle.

Every human environment is unique and, therefore, it is hard to compare and to draw general conclusions from the contact angle results. However, it is clear that the surface hydrophobicity remained fairly constant during six months *in vivo* use. This can be attributed to the silicone rubber, which is believed to be bio-stable and a good material for *in vivo* applications, e.g. for tubing purposes.

ATR-FTIR spectroscopy was performed to determine the changes in the chemical structure of the *in vivo* used samples. During the exposure, in most cases, the region of $–CH_3$ functional group (3100-2800 cm^{-1}) increased during exposure. This could be caused by the migration of low molecular weight silicone compounds to the surface, which occurred due to the degradation of the materials. In addition a new peak was detected in the region 3200 cm^{-1} and 3600 cm^{-1} in the IR spectra (Fig. 17a). This peak corresponds to the formation of Si-OH bond [108-112] that indicates the hydrolytic degradation of the material.

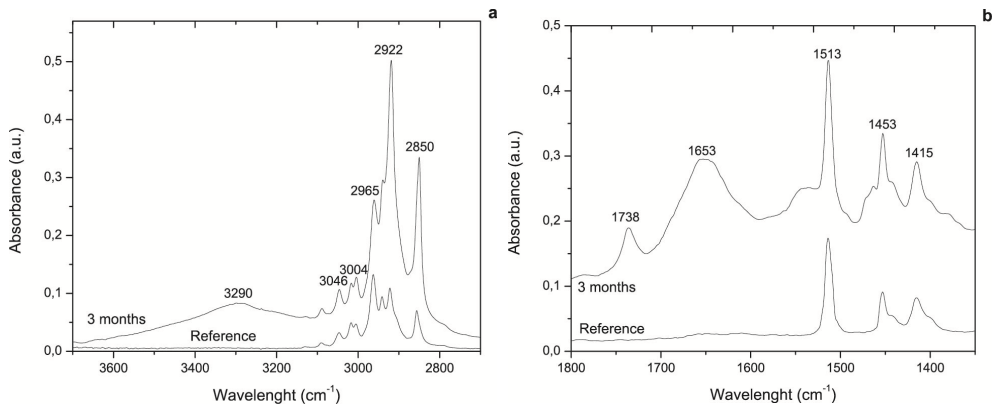

Figure 17. *Comparison of ATR-FTIR test results of an unexposed reference and in vivo used silicone rubber tracheostomy tube in region 2690 cm^{-1} to 3590 cm^{-1} (a) and 1320 cm-1 to 1720 cm^{-1} (b).*

Besides, in most of the *in vivo* used samples, new, "protein-like" peaks were observed between 1525 cm^{-1} and 1760 cm^{-1} (Fig. 17b). In this region the peaks at 1513 cm^{-1}, 1453 cm^{-1} and 1415 cm^{-1} corresponds to the ´Superslick´ coating that contain Si-Ph groups [109, 112].

Biofilm usually consists of a polysaccharide gel hosting microorganisms such as bacteria. Although the tubes were cleaned with anionic and non-ionic surfactants it is likely that some remains of the biofilm are left. The peaks, which were observed in region 1500-1800 cm^{-1} indicated presence of biofilm and traces of cell wall material from bacteria. [113-118]

MALDI-TOF MS was used to identify the molecules that are responsible for the changes of the before mentioned functional groups in the chemical structure. The mass spectra from extracts of *in vivo* samples were compared to those from reference material. Figure 18 shows

the MALDI mass spectra of an extract from a reference sample. Molecules in the m/z range 1000-2600 were detected. The difference in m/z between two adjacent peaks was m/z 74, which corresponds to the mass of one repeating unit. The molecule corresponds to this mass was found to be poly(dimethyl siloxane) (PDMS). The peaks at m/z 1059 + n·74 (n=0,1,2,…) correspond to sodium adducts of cyclic PDMS molecules. On the surface of reference sample, only cyclic PDMS molecules were found. The shortest cyclic PDMS chain was detected at m/z 1059 (14 repeating units) and the longest one at m/z 2539 (34 repeating units).

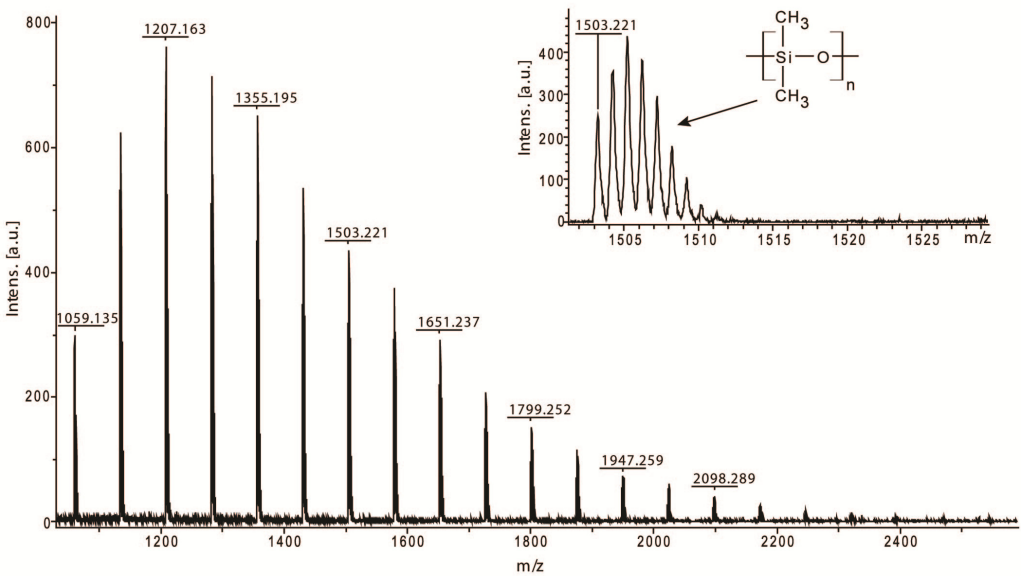

Figure 18. *MALDI TOF mass spectrum of a residue extracted from unexposed silicone rubber tracheostomy tube.*

This is somewhat surprising, as the material is comprised of both cyclic and linear PDMS. Nevertheless, the molar mass of the linear polymer is much higher (~250 000 g/mol) than that of the cyclic. MALDI sample preparation for analysis of high molar mass compounds (> ~ 50 000 g/mol) is different than that for compounds with low molar mass (> ~ 10 000 g/mol). In addition, detailed chemical structure analysis, e.g. analysis of the degree of polymerisation (DP) and end-group analysis, becomes impossible at higher molar mass due to instrumental and chemical factors, i.e. peaks originating from molecules of neighbouring DP cannot be separated due to the increasing influence of natural isotope distributions with increasing molar mass. Therefore, the aim of the current study was to focus on chemical structure analysis of low molar mass compounds in PDMS.

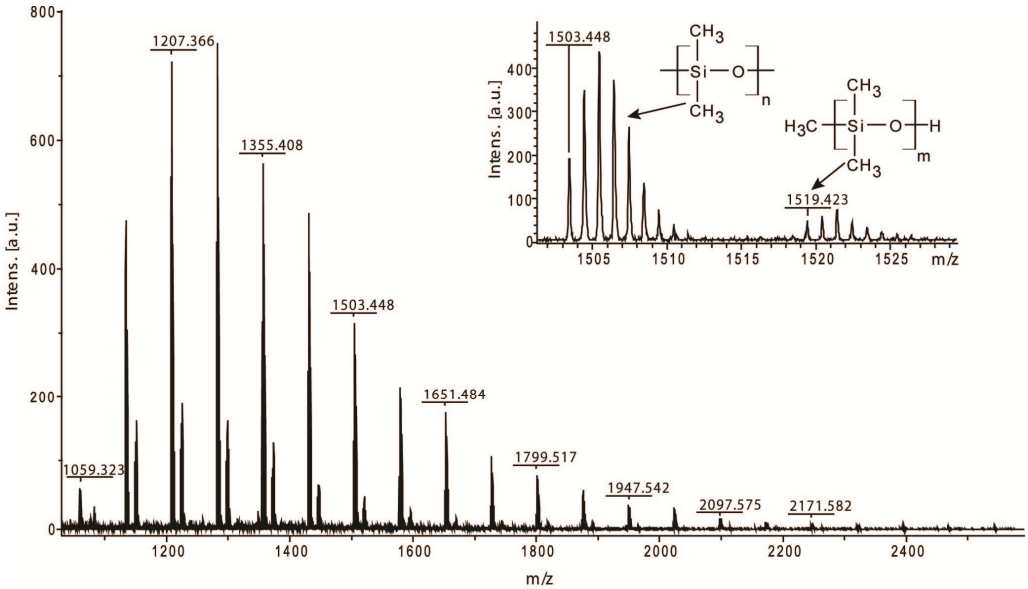

Figure 19. *MALDI TOF mass spectrum of a residue extracted from an in vivo used silicone rubber tracheostomy tube.*

Peaks at m/z +16 compared to the peaks from cyclic molecules were occasionally detected in the MALDI TOF mass spectra of extracts of *in vivo* used tubes (Fig. 19). These could originate from linear molecules with methyl and hydroxyl end groups, but could also be due to adduct formation with potassium. To rule out the possibility to potassium adducts the samples were doped with silver trifluoroacetate. In the spectra from doped samples (where silver ion adducts were detected) the m/z +16 peaks were still observed. Therefore, these peaks most likely do not originate from cyclic molecules. If linear PDMS (with methyl end groups) undergoes, hydrolysis the mass of the product oligomers will match the m/z of the unknown peaks. The cyclic PDMS is also sensitive to hydrolysis and if this should occur, peaks at m/z +18 compared to the peaks originating from cyclic PDMS would appear. However, due to overlap of the isotopic envelope, we could not detect any hydrolysis products from cyclic PDMS. Therefore, we believe that these peaks originate from linear products that formed by the hydrolysis of high molecular weight linear PDMS. Due to the hydrolysis, de-crosslinking could also occur.[108, 119] However, in the MALDI TOF mass spectra no indications on this could be detected.

It is known that some of the patients were aspirating, which could be reason for the hydrolysis. Although the backbone of the silicone rubber is stable, hydrolysis could occur (Fig. 20) in the strong acidic environment (pH ~1 – 2) originating from the gastric acid.[108, 120]

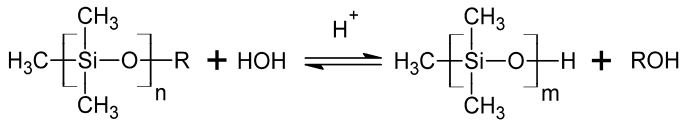

Figure 20. *Scheme of acid catalyzed hydrolysis of linear polydimethylsiloxane, where R represents next polymer or oligomer unit of the chain.*

In summary, hydroxyl-containing compounds were detected in both ATR.FTIR spectroscopy and MALDI-TOF MS. Thus, it seems clear that hydroxyl compounds were formed on the tubes during the *in vivo* exposure. The formation of these molecules confirms that the silicone rubber has been degraded by hydrolysis. Presence of biofilm on silicone surfaces has been demonstrated in other applications, e.g. outdoors high voltage insulators [118]. Once a surface has been in contact with water, inorganic and/or organic particles a colonisation of microorganisms occur. The environment at the interphase between a biofilm and a polymeric surface could be very aggressive and combinations of degradation mechanisms most likely combine resulting in chemical and/or biological degradation. Even if silicone is inert to biodegradation, the biofilm formation resulted in a slow hydrolysis and a change in surface characteristics that may lead to a decreased lifetime of the material in question.

4.4 IN VITRO DEGRADATION OF ANTIMICROBIAL COMPOSITES

4.4.1 Degradation of polyurethane composites

It was shown in the *in vivo* studies that surface degradation of polymers occurs as a function of time. During exposure of TPU and PEU composites to artificial body liquids similar surface alterations were observed. Pure urethane samples showed surface changes as a function of time in both ALF and Gamble solution (Fig. 21). As a result, the surface roughness increased and smaller degradation signs (cracks, holes) appeared on the surface. Some of these changes can originate from manufacturing and preparation of the samples. It must be highlighted that on the surface of Gamble aged samples, high amount of salt residues were also found.

On the surface of zeolite-polyurethane composites obvious degradation signs were identified (Fig. 22). As a function of time and zeolite content an increasing amount of small holes were observed on the surface of ALF exposed samples. These holes started to form after 1 month and their formation increased intensively during the whole exposure. Since the dimension of the holes is between 2-4 microns, it is thought that zeolite particles diffused out of the materials by leaving such a cavity behind. The highest amount of cavities was found on the surface of samples that contained Ag ions and 5 % zeolite.

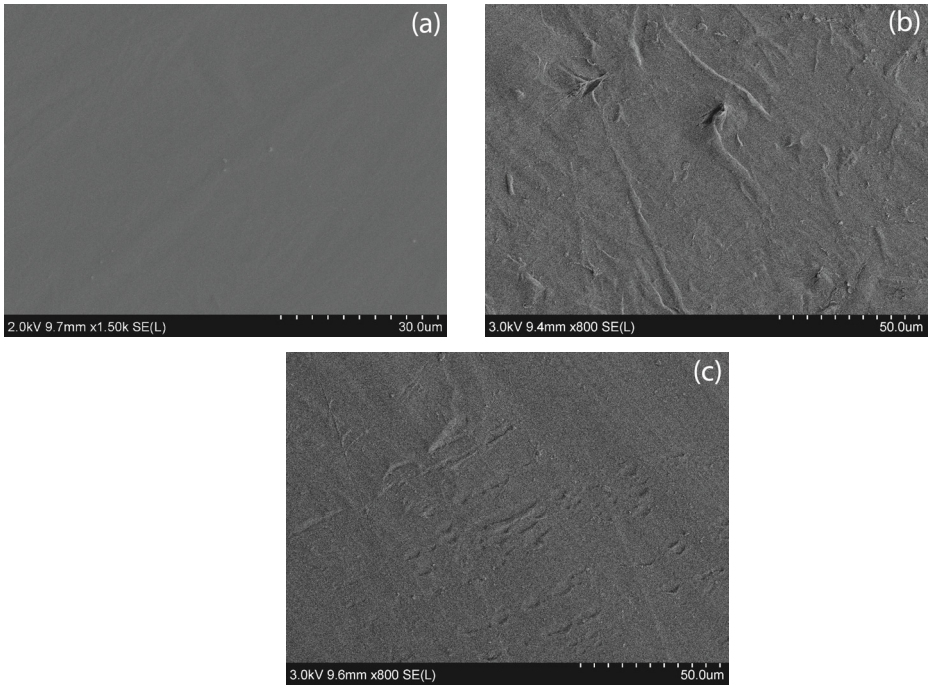

Figure 21. *SEM micrographs of the surface of unaged pure and aged TPU in ALF (b) and Gamble´s (c) solution for 3 months.*

It can be explained by the high ion-exchange activity of silver in zeolites. It is known that silver exchanges easily with other ions in the environment. Therefore besides the concentration gradient, the high activity of silver can increased the diffusion of zeolite to the surface. This surface alteration was found on non-silver containing composites (zinc, copper) and also on the surface of zeolite-TPU composites that were not filled with any ions. This indicates that apart from the activity of the ion, the zeolite itself is capable to diffuse to the surface of the polymer and migrate out in order to form equilibrium between the bulk and the environment.

In case of Gamble aged samples the before mentioned cavities were found irregularly on the surface of different samples. The shape of these surface alterations was not uniform and they seemed to be caused by erosion. In addition high amount of salt remained on the surfaces after cleaning. The reason for this could be that the different salts from the Gamble solution interacted with the surface of the polymer and bonded to the surface structure or reacted with the ions of the zeolite on the surface and stuck there afterwards. This salt layer can highly influence the ion and zeolite release from the composites and their hydrophobicity as well.

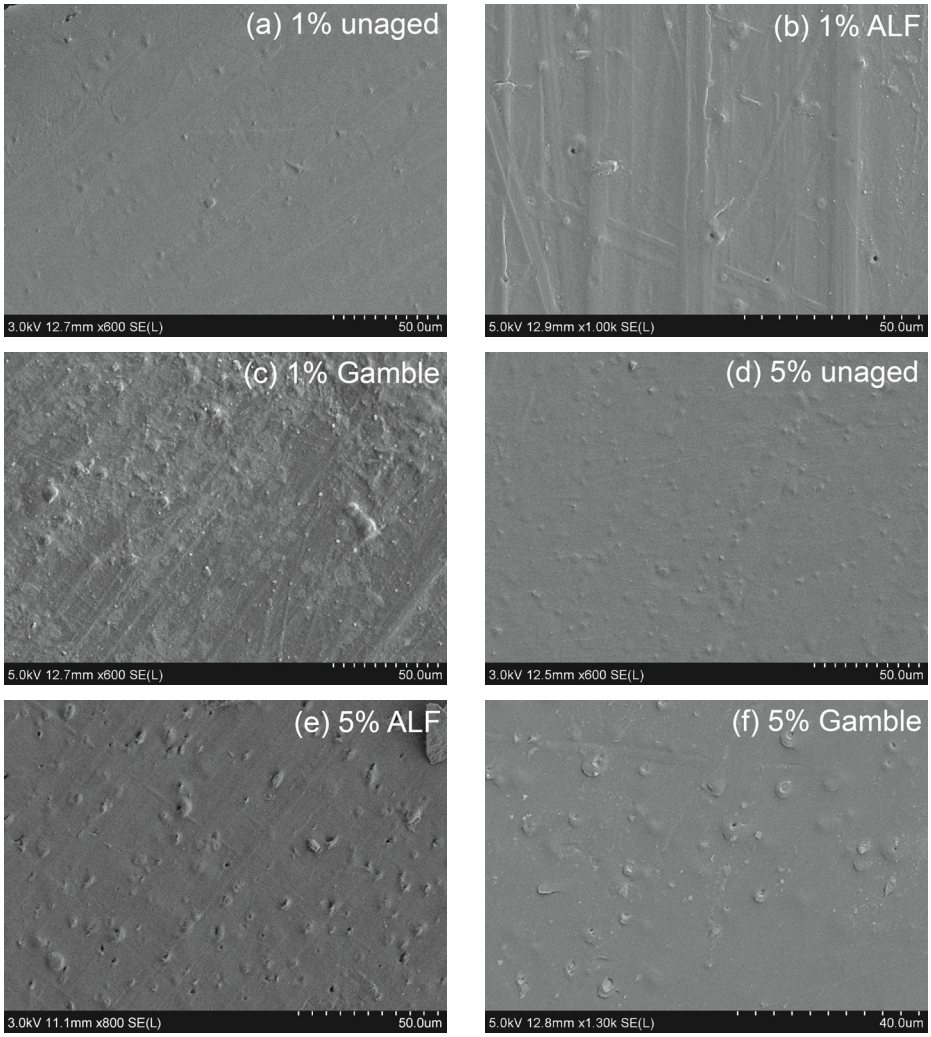

Figure 22. *SEM micrographs of the surface of unaged, ALF and Gamble exposed 1 and 5% zeolite PEU.*

Figure 23 and 24 represents the contact angle change of zeolite-TPU and zeolite-PEU as a function of exposure time in the ALF and Gamble's solutions are presented. No significant differences in the decrease trend of contact angles were detected for the samples exposed to the ALF or the Gamble's solution.

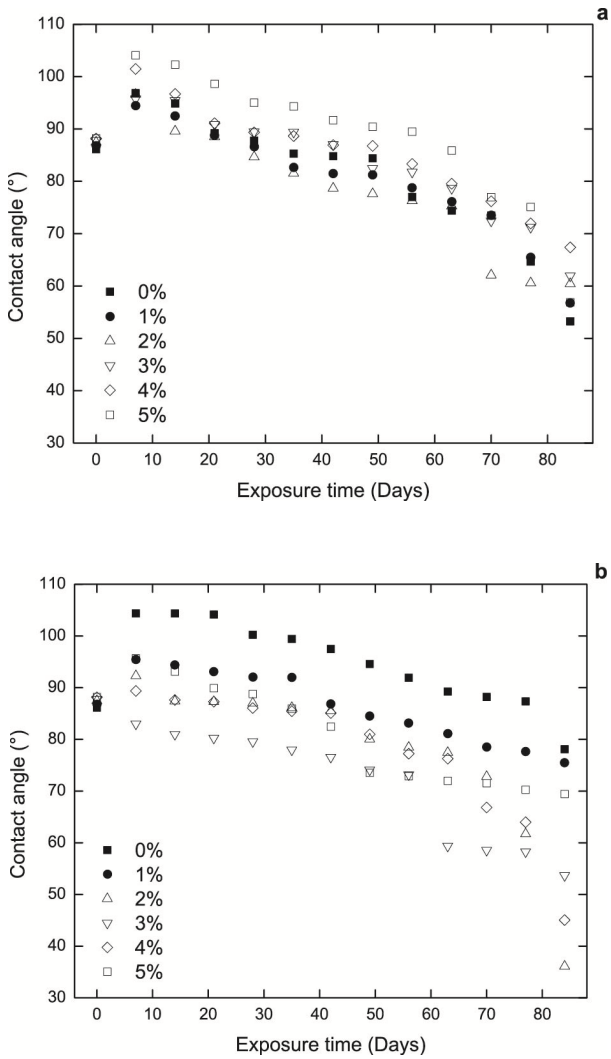

Figure 23. *The contact angle change of TPU-zeolite composite samples with increasing zeolite content as a function of exposure time in ALF (a) and Gamble´s solution (b).*

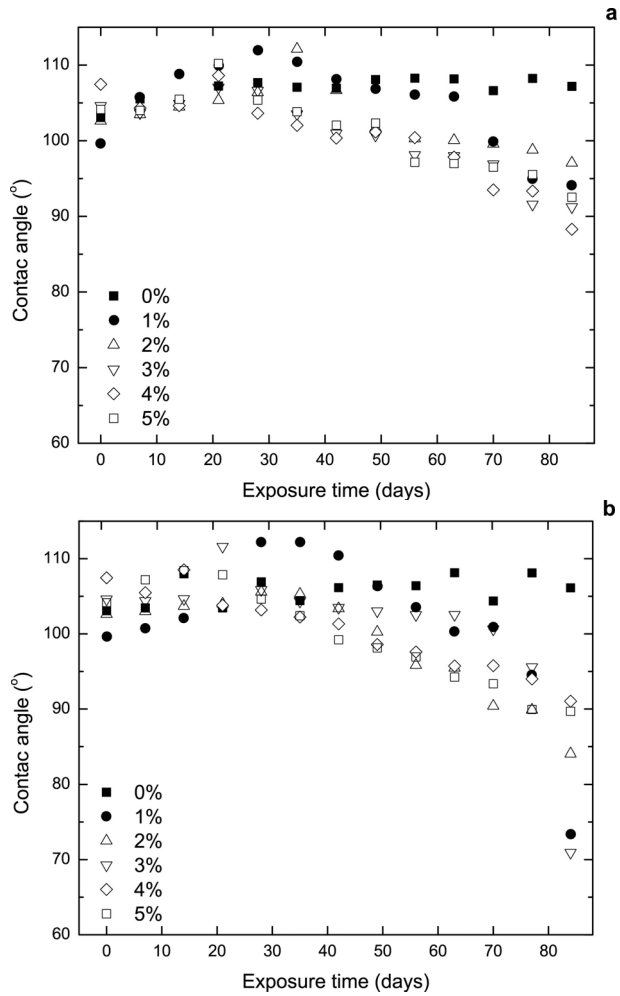

Figure 24. *The contact angle change of PEU-zeolite composite samples with increasing zeolite content as a function of exposure time in ALF (a) and Gamble´s solution (b).*

As can be seen from Figure 23 and 24, the contact angle of both polyurethanes increased and reached a maximum value. For TPU this value was observed after 7 days while for PEU the increase of the contact angle increased up to 21-35 days. After this point the contact angle decreased during the remaining time of the exposure. In case of TPU composites the decrease of the contact angle could be distinguished into different stages. The first stage was found to be between 7-28 days. After the contact angle reached a maximum value, it started to decrease. This was followed by a semi-stationary stage 28-49 days in ALF solution and 28-35 days in Gamble´s solution where the values of the contact angle decreased with a lower rate. This was clearly visible for samples exposed to the ALF solution. Then the contact angle

decreased with the same intensity as during the first stage for the remaining period of the test. The phenomena that caused the observed plateau are believed to consist of three stages. In the first stage, TPU absorbed water until it at a certain point (around 28 days) reached its´ maximum water uptake capacity. During the second stage, where a slight decrease was observed, TPU could not absorb more water and the degradation process was initiated. At stage three, i.e. in ALF solution after 49 days and Gamble´s solution after 35 days, the contact angle again started to decrease as a result of the degradation of TPU with a resulting change in the chemical structure of the material.

For PEU the decrease of contact angle occurred only in one stage after it reached the maximum value. No plateau was observed. In addition in case of TPU the contact angle of the pure TPU decreased as a function of time while for PEU it slightly increased in the beginning and after 14 days it became constant and did not change during the whole aging process in any of the solutions. This can be linked to the structural differences in between the two polyurethanes. Polyether type polyurethanes are known to be more stable against aging environment than polyesters. This indicates that polyesters degrading with a higher rate on exposure. Compared to the initial value, the final contact angle of TPU showed a bigger decrease than the PEU, which confirms this theory. In the beginning the surface of both polyurethanes were hydrophobic, however due to the aging the TPU lost its hydrophobicity after 21 days already while PEU remained hydrophobic after the complete exposure in ALF solution. In Gamble solution this materials also lost its´ hydrophobic behaviour after 10 weeks exposure. It can be concluded from the results that as it was observed on the SEM micrographs, significant change in the surface structure has occurred. This change seemed to be influenced by the zeolite concentration. This is due to that both polyurethanes absorb moisture and zeolite is highly hygroscopic. Therefore the water absorption of the zeolite-TPU composites is increasing with the increased zeolite content. This water uptake is a reasonable explanation for the significant decrease in the contact angle, since more aging solution can reach the bulk and initiate degradation processes. However for the initial contact angle increase can be explained either by the migration of low molecular weight compounds, or other hydrophobic additives, from the bulk of the material or by the chemical changes in the surface structure due to the aging solutions. This chemical change could result the formation of hydrophobic groups on the surface that can be responsible for the increased contact angle.

In order to study the chemical changes that cause this behaviour of the contact angle, FTIR was performed weekly on the samples. The obtained infrared spectrum of both *in vitro* aged polyurethanes showed significant changes in the chemical structure. The IR spectrum of TPU and PEU is quite similar. The only difference is due to the ester and ether bond.

The region of N-H (3200-3500 cm^{-1}) and -CH2- (3000-2800 cm^{-1}) stretching for TPU and PEU is presented in Figure 25-26. In general the area of -CH2- increased in both polyurethane

samples. In case of TPU this functional group slightly increased as a function of exposure time, while for PEU the area of -CH2- increased up to 28-42 days and started to decrease afterwards. The most significant increase of -CH2- was observed for pure-PEU. In addition the area of -CH2- for this sample remained constant after the initial increase.

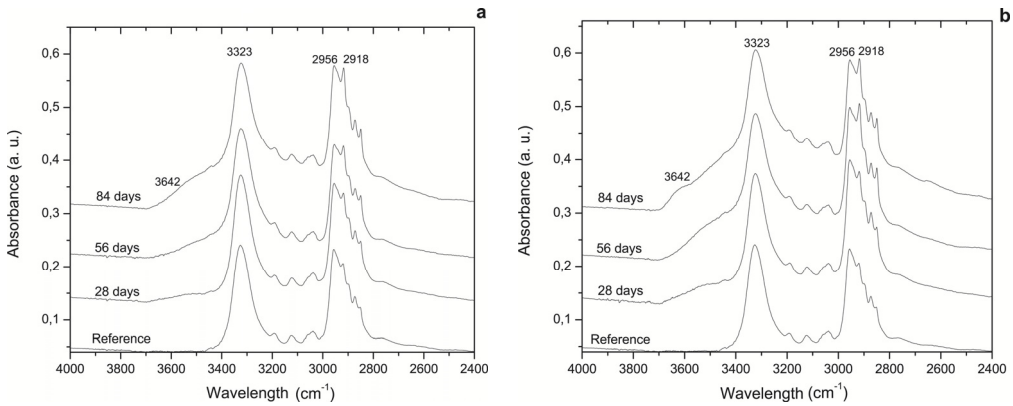

Figure 25. *The comparison of the ATR-FTIR spectrum of pure (a) and 5 % zeolite containing TPU (b) at different exposure times in Gamble´s solution in region 4000-2400 cm^{-1}.*

This region of -CH2- represents the bonds of polyester (TPU), polyether (PEU) and cyclohexane and the increase indicates the formation of these compounds. It is known that cyclic alkanes are hydrophobic. This may be the responsible for the initial contact angle increase in the samples. The formation of these compounds started right after one-week exposure and reached a maximum level shortly. This observation matches well with the contact angle results of the polyurethane composites, where the maximum value was also reached in 7-28 days and then a decreasing tendency was observed.

Besides the increase of -CH2-, the formation of –OH groups was also detected in the region 3400-3700cm^{-1} for both polyurethanes. This peak started to form after one week and increased slightly as a function time in both aging solutions. The formation of –OH groups indicates oxidative degradation of the soft segment. In addition in Gamble solution apart from the pure TPU, the –OH peak broadened and formed an overlap with the N-H region in PEU after 4 weeks exposure while this overlap was observed for TPU after 12 weeks. The intensity of this peak found to be influenced by the zeolite content. It was reported in the literature before, that the N-H region may overlap with the region of the –OH group [40, 121-123] that indicates oxidative degradation and the formation of hydrogen bonds as well [35, 124, 125].

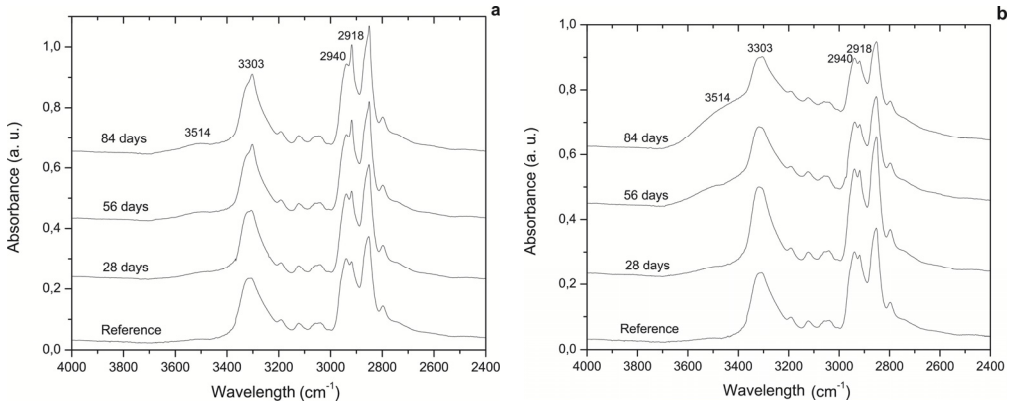

Figure 26. *The comparison of the ATR-FTIR spectrum of pure (a) and 5 % zeolite containing PEU (b) at different exposure times in Gamble´s solution in region of 4000-2400 cm^{-1}.*

During the oxidative degradation of the hard segment bond scission takes place on the urethane linkage, which indicates the broadening of the N-H region and is due to the formation of primary amines. In addition, since the carbonyl groups are attached to the N-H group by hydrogen bonds in the polymers hard segment, the formed shoulder between the N-H and –OH group can also correspond to the increase of this bond. Due to the fact that N-H has and overlap with the OH clear evidence on the increasing hydrogen bonds can only be concluded from the carbonyl ratios.

It has previously been reported that the high elasticity and strength of the polyurethanes is due to the hydrogen bonding between N-H and C=O groups in the hard segment of the material. However, besides the H-bounded C=O groups, free C=O groups (non-H bounded) are also present in the material [40]. Due to this, the change in the number of the H-bonds can be monitored by the peak intensity ratios of the H-bounded C=O groups and free C=O groups. The formation of free C=O groups indicates the cleavage of H-bounded C=O groups, which may result from oxidation of the material while the increase of bounded carbonyl groups corresponds to the formation of new hydrogen groups between the hard and the soft segments.

In case of TPU, during the exposure in both *in-vitro* ageing solutions the free C=O peak at 1726 cm^{-1} increased as a function of time and zeolite content, while the bounded C=O (1699 cm^{-1}) didn't change (Fig. 27). This indicates that the H-bounded/free C=O group ratio decreased. This change was increased as a function of zeolite content and indicates the oxidative degradation of TPU during the exposure.

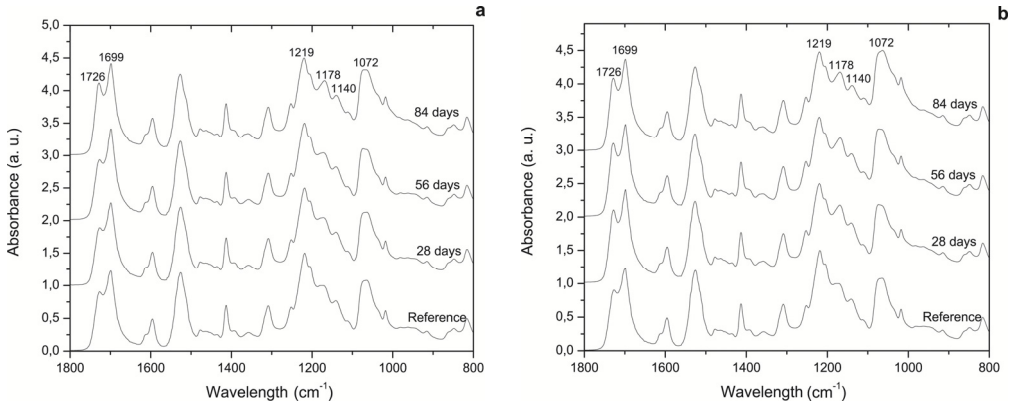

Figure 27. *The comparison of the ATR-FTIR spectrum of pure (a) and 5 % zeolite containing TPU (b) at different exposure times in Gamble´s solution in region of 1800-800 cm^{-1}.*

For PEU the opposite of this phenomenon was observed (Fig. 28). In this material the hydrogen-bonded carbonyl appears at 1697cm^{-1} while the free C=O can be found at 1727cm^{-1}. The bonded/free carbonyl ratio increased as a function of time that indicates the formation of new hydrogen bonds. This increase was caused by both the increase of the bonded C=O and the decrease of the free C=O. This change indicates that most of the free carbonyl groups present in the system bound to the N-H of the hard segment. The intensity of this change in the chemical structure was the same for pure PEU and PEU composites up to 3 % zeolite. Above this amount more intense alteration of the FTIR spectrum was observed [40]. In general no difference was seen between the polyurethane samples aged in ALF or Gamble´s solution.

Apart from the change in the same functional groups, changes in the TPU-s polyester and PEU´s polyether linkage was also observed.

The polyester bond of TPU can be found at 1178 cm^{-1}. This peak increased as a function of exposure time in both aging solutions and was slightly influenced by the zeolite content. The increase of the ester functionality suggests oxidative degradation of the material, which was confirmed by the changes in the other functional groups of TPU as well [40, 123, 125, 126].

In case of PEU for samples that contained more than 3 % zeolite the C-O-C asymmetric stretching of polyether (1103 cm^{-1} and 1070 cm^{-1}), urethane (1017 cm^{-1}) and the asymmetric ring stretching of the cyclohexane increased significantly [124]. In addition the peak at 1368 cm^{-1} that corresponds to the poly(tertamethylene glycol) decreased as a function of time. This gives evidence and confirms that oxidative degradation and bond scissions occurred in both the hard and soft segment with increased functionality of ether and aromatic groups.

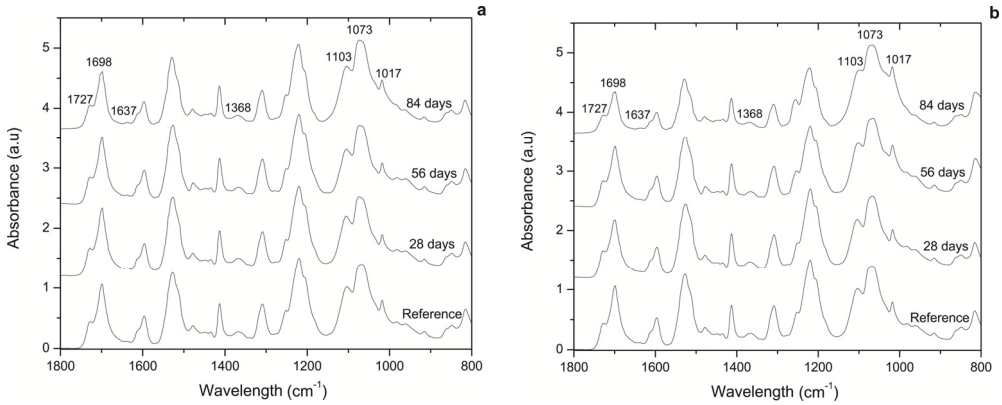

Figure 28. *The comparison of the ATR-FTIR spectrum of pure (a) and 5 % zeolite containing PEU (b) at different exposure times in Gamble´s solution in region of 1800-800 cm^{-1}.*

In summary the FTIR results confirmed that chemical changes occurred in both polyurethanes during exposure to both the ALF and the Gamble's solutions. The change in chemical the structure is a result of oxidative degradation caused by the artificial body fluids and the zeolite content has shown to have influence on the degradation. This is due to the increasing zeolite content, which results that, the water uptake of the composites increases. This indicates an increase in the amount of solution penetrating into the bulk and thereby an increased degradation rate.

4.4.2 Degradation of silicone rubber

The contact angle measurements performed on the silicon rubber samples revealed similar changes in the beginning of exposure as in the case of the TPU samples (Fig. 29). The contact angle increased after 7 days, reached a maximum value and started to decrease as a function of time in both artificial fluids. The change was, however, more intense for the samples exposed in Gamble´s solution where the surface of some samples became hydrophilic after 84 days. The obtained change seemed also to be less influenced by the zeolite content. However, due to the zeolite addition the water uptake of the silicone rubber may increase.

The FTIR spectra of silicone showed indications of changes in the chemical structure of the material, especially in the case of the samples exposed in the ALF solution (Fig. 30). In both artificial fluids the peaks at 1152 cm^{-1} and 1207 cm^{-1}, which correspond to the cross-linked (bonded by –CH2-) section of silicone rubber, slowly decreased as a function of time and zeolite content (Fig. 30a). This indicates that de-cross-linking is taking place in the material.

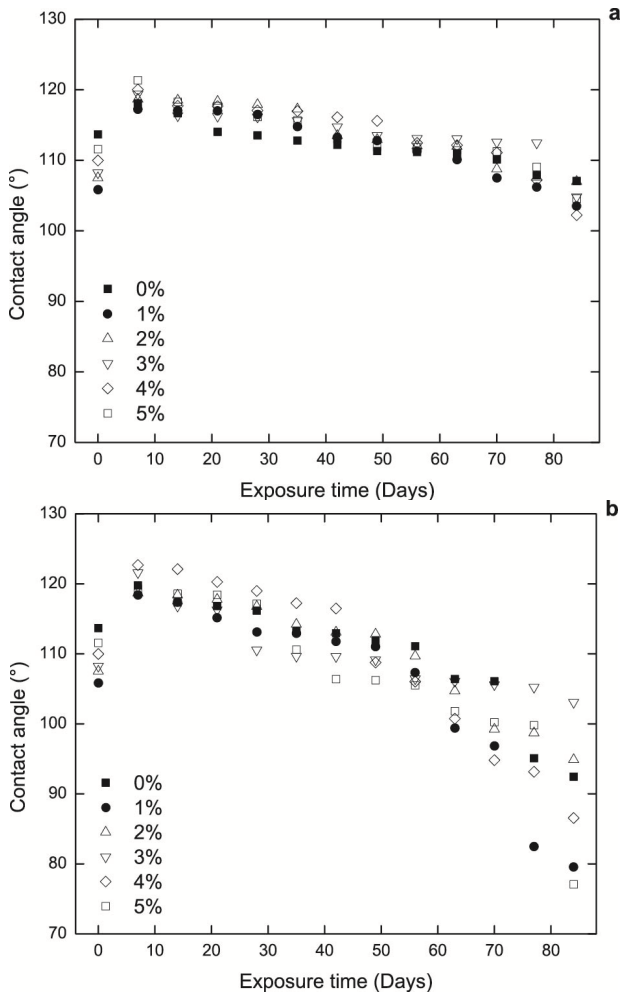

Figure 29. *Measured contact angle as a function of exposure time for samples of zeolite-silicon rubber exposed for 84 days in (a) ALF solution and in (b) Gamble's solution.*

In Figure 30b the FTIR spectrum of the OH region of the silicon rubber samples is presented. As can be seen from the figure, a peak appeared in the region between 3700-3550 cm^{-1} after 84 days of exposure in both artificial fluids. The peaks were identical to those identified in the PU spectrum, which corresponds to the formation of hydroxyl groups. The formation of the Si-OH peak indicated that hydrolysis was taking place in silicone rubber [108, 109]. The increasing intensity of the Si-OH bonding as a function of zeolite content revealed that the silicone rubber samples had absorbed an increasing amount of water as a result of the zeolite addition. This phenomenon was also observed for the zeolite-PU samples. As a result of this

observation it can be concluded that the zeolite addition leads to a similar initiation of degradation in both PU and silicon rubber.

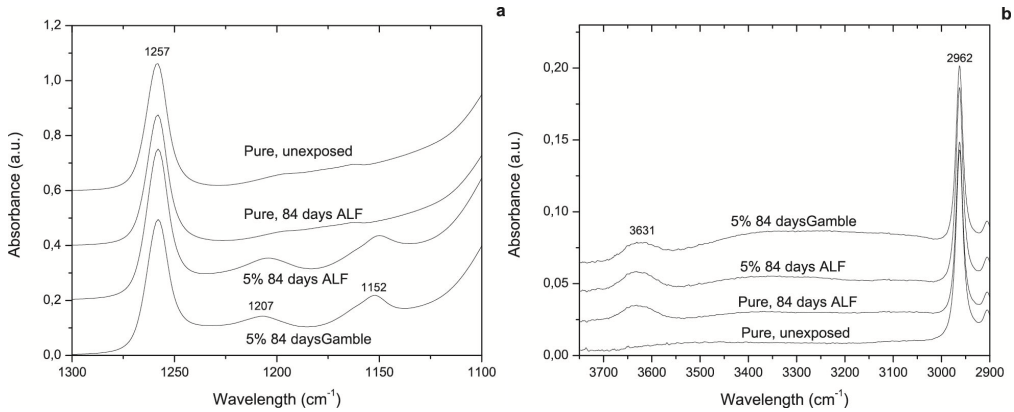

Figure 30. *FTIR spectrum of the –CH2- (b) and -OH- (a) region: (a) for silicone with 5% zeolite exposed for 84 days in the Gamble's solution, (b) for silicone with 5% zeolite exposed for 84 days in the ALF solution, (c) for pure silicone in the ALF solution, and (d) for pure silicon as a reference.*

MALDI-TOF-MS measurements were performed on the silicone rubber samples in order to detect changes in the chemical structure due to the exposure. In case of PU it was not possible to conduct MALDI-TOF-MS measurements as PU consists of two segments, which need to be separated prior to the analysis. There have been a few studies referring to MALDI analysis of PU where the hard and soft segments were separated by selective degradation reactions [92, 93]. In the present case, the degradation products played a vital role in the understanding of the degradation phenomenon during *in-vitro* ageing of PU. As a result, the selective degradation reactions might have influenced the degradation products of the *in-vitro* aged samples.

In the unexposed silicone two silicone compounds were identified. One series of peaks was detected at m/z 1133 + n·74 (n=1,2,3,…) which corresponds to cyclic poly(dimethyl siloxane) (PDMS) molecules with sodium ion adducts. The m/z difference between two adjacent peaks in this series was 74, which corresponds to the mass of one repeating unit in PDMS the same molecule was identified to be the repeating unit of silicone tracheostomy tubes. Peaks corresponding to dimethyl terminated linear PDMS were observed at m/z 1147 + n·74 (n=1,2,3,…). The peak of this linear PDMS was Δm/z +14 compared to the cyclic compound, which is due to the additional two methyl end groups to Si atoms on both ends of the chain.

In Figure 31 the MALDI-TOF MS spectra of silicon rubber with 5 % zeolite (exposure times: 0, 28, 56 and 84 days in Gamble´s solution) is plotted. As can be seen from

the figure, the peak intensity ratio between the cyclic and the linear compound increased as a function of time, and after 28 days an overlap appeared on the spectra. This indicates the formation of another linear compound. Since the third isotope peak has the highest intensity and the intensity of the following peaks shows uneven distribution, this peak is the first isotope peak of the newly formed compound. Therefore, the Δm/z shift for this compound is +16 compared to the cyclic PDMS which indicated the formation of linear PDMS with methyl and hydrogen (O-H) end groups. The formation of this silicone compound was also observed during the *in vivo* degradation of silicone rubber tracheostomy tubes [127].

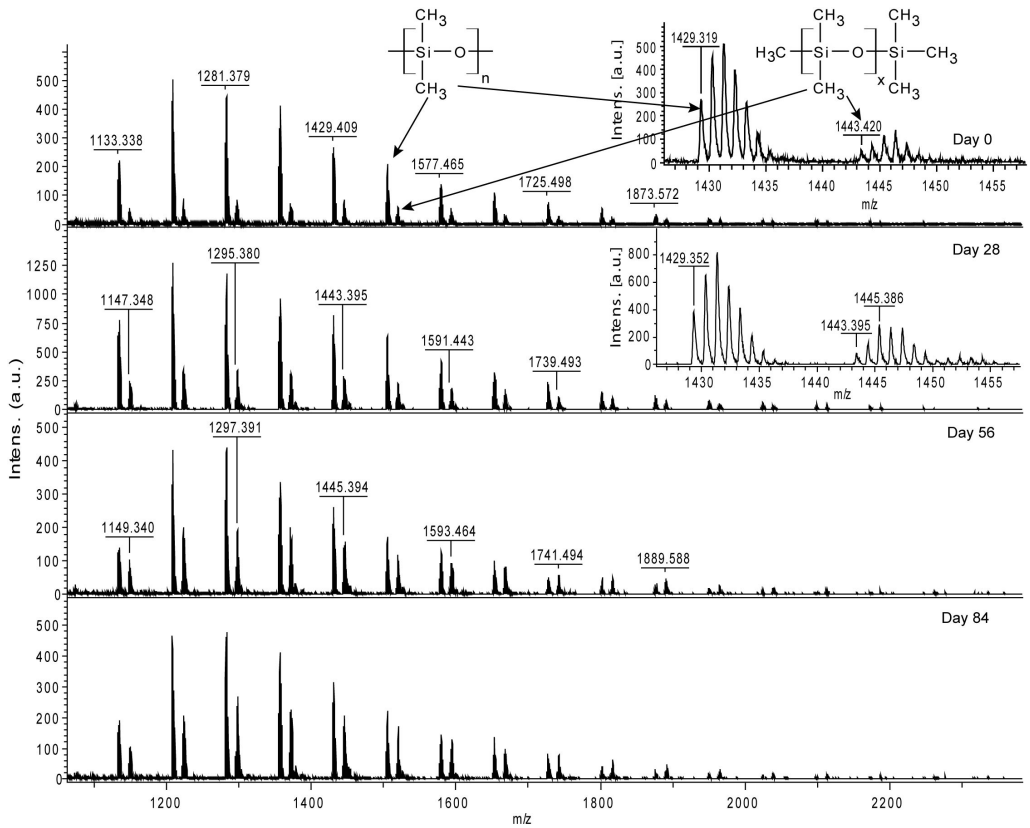

Figure 31. The MALDI-TOF MS spectra of silicone rubber with 5% zeolite in Gamble´s solution after 0, 28, 56 and 84 days of exposure.

Figure 32 represents the detected and calculated isotope distribution pattern for dimethyl terminated and methyl, hydrogen terminated PDMS. The calculated data correlates well with the detected isotope pattern, and confirms the formation of methyl, hydrogen PDMS after 28 days.

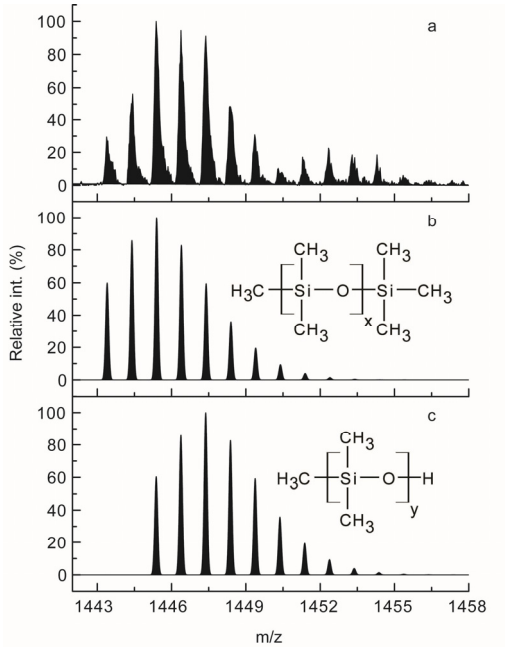

Figure 32. *Detected (a) and measured isotope pattern for (b) dimethyl and (c) methyl, hydrogen terminated PDMS.*

MALDI-TOF MS is a technique that is capable of providing semi-quantitative information about the compounds in question under certain circumstances.[128-130]. For the two types of compounds of interest in the present study the peak intensity ratio could be used to estimate the change in relative composition. The intensity of the linear PDMS molecule increased as a function of time that indicates the continuous formation and increasing concentration of new molecules in the material (see Fig. 31).

The MALDI TOF results correlate well with the obtained FTIR results where the OH region of the material increased as a function of exposure time while the crosslinked area completely disappeared. It is a well known fact that degradation of silicone can occur by hydrolysis [3, 108], and that it results in an increased concentration of the hydroxyl group in the samples.

In summary, both the FTIR and the MALDI-TOF MS results confirmed the formation and increasing concentration of linear PDMS with dimethyl and methyl-hydrogen end-groups in silicone rubber. This clearly indicates the existence of both de-crosslinking and hydrolyses of the material.

5 CONCLUSIONS

It was demonstrated that although silicone rubber is regarded as inert and biocompatible as biomedical material a slow degradation occurred during the use of tracheostomy tubes for periods up to six months. The degradation process was initiated already after one-month exposure and resulted in significant changes in the material after six months. This was due to a complex combination of biofilm formation on the surface and the human body fluid itself. As a result of the degradation low molecular weight compounds were formed due to the hydrolysis of the silicone rubber.

The preparation of new antimicrobial filler was successful. The fillers were binary and ternary ion-exchanged zeolites loaded with Ag, Cu and Zn ions. Due to the differences in the hydrated ionic radius, the activity of ions and the preference of the zeolite structure the different ions absorbed with various amounts in the crystal. Silver was the most preferred by the zeolite and it was followed by the zinc and copper. All three ions are competing to bond to the same place in the crystal, resulting in multi-ionic systems with the different ions concentrated at one location in the crystal. This influenced the ion release since if a more preferred ion is located on the outer part of the crystal it blocks the way of other ions that can be easily exchanged. Zinc was released with the highest amount and it was followed by the copper and silver ions.

The antimicrobial tests showed that silver ion exchanged zeolite was superior to the other samples. In addition the antimicrobial efficiency of the Ag-Zn and Zn-Cu samples demonstrated some potential therefore these materials may have a perspective.

The surface properties of the composites were slightly influenced by the zeolite content. The tensile strength and the elongation of the composites decreased with the increase of the zeolite content. The Young´s modulus decreased for the polyurethane composites and increased for silicone rubber.

The zeolite content had a positive influence on antimicrobial activity of the composites. The multi-ionic systems silver exchanged composites was superior to the other samples. Binary and ternary ion exchanged zeolite composites showed similar antimicrobial efficiency while Cu and Zn exchanged samples did not show any effect.

The *in vitro* (artificial body fluid) ageing showed that the probable degradation mechanism of polyurethane composites was oxidation while hydrolysis was observed for the silicone rubber. The degradation process for TPU and PEU composites were similar, the main difference is in the scission of the hydrogen bonds between the soft and hard segment and in the polyether, polyester bonds.

6 FUTURE WORK

The future work of this study will aim to improve the currently used and develop new in vitro environments in order to get a better inside of specific degradation processes that may occur in the human body either due to body fluids, or microbiological environment.

It is also important to prove the antimicrobial efficiency and in vitro stability of the currently used composites through clinical evaluation and in vivo trials.

Besides, the development of alternative antimicrobial agents has high importance and great perspective in several industrial areas. This research would aim to eliminate synthetic materials as antimicrobial agents and developing more biologic friendly materials that have an increased and sustainable antimicrobial effect.

Furthermore the possibility of the currently used composites for other industrial applications than the medical field must be examined, since based on the antimicrobial performance these materials have a potential in other applications as well where the outer environment is less aggressive than the human body.

7 ACKNOWLEDGEMENTS

First I would like to express my deepest gratitude to my main supervisors, Prof. Sigbritt Karlsson (KTH) and Dr. György Czél (University of Miskolc) for accepting me as a PhD student and for the continuous support I got from them during my work. I would like to thank my secondary supervisors Prof. Ragnhild E. Aune, Dr. Emma Strömberg and Dr. Dane Momcilovic for contributing with their expertise in my research. Special thanks to Emma for her friendship, for always being there and helping me so much both at work and in private life.

The senior members of our division; Prof. Ulf Gedde, Prof. Mikael Hedenqvist, Doc. Henrik Hillborg and Assistant Prof. Richard Olsson are acknowledged for their technical help and for making the department an inspiring place to work at.

I am grateful for the financial support given me by VR and KTH. Further Anikó Guba and the Hungarian National Public Health and Medical Officer Service are thanked for assisting in the microbiological tests and for providing microorganism strains, laboratory and the necessary equipments. Dr. Ralf Schnell from Tracoe GmBH is gratefully acknowledged for the valuable discussion that set the main directions of the project and for the raw material that was supplied by his company. I am thankful to Zoltán Márkus at University of Miskolc for helping me a lot with the samples preparations and being there to support even at nights and to Catharina Silfwerbrand for her technical support.

I would like to thank the ex-SK group members: Åsa for trying to improve my Swedish, Jonas for the great innebandy games and support in MALDI, Fran for being the pioneer in taking a joint PhD.

I am grateful to Sevil for being always happy and cheer me up when I was not in the mood. I thank Thorsak for being so funny and being such a nice person. I am indebted to Hasan, Sohail and Thomas for being my friends and for the great times we spent together. Special thanks go out to “Prof.” Bayley for showing the SA way of life and for the language corrections he applied on this work. I would like to thank my other dear colleagues Anna, Bwire, Erik, Dahlia, Fredrik, Fritjof, Henrik, Louise, Minoo, Nima, Patricia, Petra, Sara, Wenbin, Wen-Chung. I would also like to thank all the other department members who contributed in my work, the guys at innenbady and Andreas, Carl, Nicholas for the great tennis matches. I am also thankful to my former exam worker Mar M. Pérez-Madrigal.

Külön köszönet illeti szüleimet és párjaikat, húgomat, nagyszüleimet, keresztszüleimet és unokatestvéremet. Köszönöm nektek a rengeteg bíztatas, támogatást és bátorítást amit

kaptam, azt hogy mindig mellettem álltok. Nélkületek nem lennék most itt és nem sikerült volna.

Finally I would like to thank Dora for her endless love, support and encouragement. Thank you for your patience and loyalty in the hard times. It meant a lot to me!

8 REFERENCES

[1] Williams D. F.: The Williams Dictionary of Biomaterials Liverpool: Liverpool University Press (1999).

[2] Dorland W. A. N.: Dorland's Medical Dictionary Philadelphia, Pennsylvania, USA: W.B. Saunders Company (1980).

[3] Akmal N., Usmani A. M.: Medical polymers and diagnostic reagents, in ´Medical polymers and diagnostic reagents´ (ed.: Hamid S.) Marcel Dekkel Inc., New York, 485-495 (2000).

[4] Gebelein C. G.: Medical Applications of Polymers, in ´Applied Polymer Science´, 535-556 (1985).

[5] Hofmann D., Entrialgo-Castaño M., Kratz K., Lendlein A.: Knowledge-Based Approach towards Hydrolytic Degradation of Polymer-Based Biomaterials. Advanced Materials (Weinheim, Germany), **21**, 3237-3245 (2009).

[6] King R. N., Lyman D. J.: Polymers in Contact with the Body. Environmental Health Perspectives, **11**, 71-74 (1975).

[7] Venkatraman S., Boey F., Lao L. L.: Implanted cardiovascular polymers: Natural, synthetic and bio-inspired. Progress in Polymer Science, **33**, 853-874 (2008).

[8] Lynch J. F., Lappin-Scott H. M., Costerton J. W.: Microbial biofilmsCambridge: Cambridge University Press (2003).

[9] Strömberg E.: Microbiological growth testing on silicone rubber materials, in Fibre and Polymer Technology, Royal Institute of Technology: Stockholm (2004).

[10] Flemming H.-C.: Relevance of biofilms for the biodeterioration of surfaces of polymeric materials. Polymer Degradation and Stability, **59**, 309-315 (1998).

[11] Mayer C., Moritz R., Kirschner C., Borchard W., Maibaum R., Wingender J., Flemming H.-C.: The role of intermolecular interactions: studies on model systems for bacterial biofilms. International Journal of Biological Macromolecules, **26**, 3-16 (1999).

[12] Beech I. B.: Corrosion of technical materials in the presence of biofilms--current understanding and state-of-the art methods of study. International Biodeterioration & Biodegradation, **53**, 177-183 (2004).

[13] Wallström S., Dowling K., Karlsson S.: Development and comparison of test methods for evaluating formation of biofilms on silicones. Polymer Degradation and Stability, **78**, 257-262 (2002).

[14] Wallström S., Strömberg E., Karlsson S.: Microbiological growth testing of polymeric materials: an evaluation of new methods. Polymer Testing, **24**, 557-563 (2005).

[15] Seal K. J., Morton L. G. H.: Chemical Materials, in ´Chemical Materials´ (ed.: Schönborn W.) VCH, Dusseldorf, 583-606 (1986).

[16] Wallström S.: Biofilms on silicone rubber materials for outdoor high voltage insulation, in Department of Fibre and Polymertechnology, Royal Institute of Technology: Stockholm (2005).

[17] Sand W.: Microbial Mechanisms of Deterioration of Inorganic Substrates- A General Mechanistic Overview. International Biodeterioration & Biodegradation, **40**, 183-190 (1997).

[18] Albertsson A. C., Karlsson S.: Chemistry and biochemistry of polymer biodegradation, in ´Chemistry and biochemistry of polymer biodegradation´ (ed.: Griffin G. J. I.) Springer, New York, 7-17 (1994).

[19] Karlsson S., Albertsson A.-c.: Biodegradable polymers and environmental interaction. Polymer Engineering and Science, **38**, 1251-1253 (1998).

[20] Williams D. F.: Mechanisms of biodegradation of implantable polymers. Clinical Materials, **10**, 9-12 (1992).

[21] Williams D. F.: Interfacial reactions in the degradation of polymers by cells and bacteria. Biofouling: The Journal of Bioadhesion and Biofilm Research, **4**, 225 - 230 (1991).

[22] Kaali P., Momcilovic D., Markström A., Aune R., Czel G., Karlsson S.: Degradation of biomedical polydimethylsiloxanes during exposure to in vivo biofilm environment monitored by FE-SEM, ATR-FTIR, and MALDI-TOF MS. Journal of Applied Polymer Science, **115**, 802-810 (2010).

[23] Gumargalieva K. Z., Moiseev Y. V., Daurova T. T., Voronkova O. S.: Effect of infections on the degradation of polyethylene terephthalate implants. Biomaterials, **3**, 177-180 (1982).

[24] Lyu S.Untereker D.: Degradability of Polymers for Implantable Biomedical Devices. International Journal of Molecular Sciences, **10**, 4033-4065 (2009).

[25] Göpferich A.: Mechanisms of polymer degradation and erosion. Biomaterials, **17**, 103-114 (1996).

[26] Lukasiak J., Dorosz A., Prokopowicz M., Rosciewski P., Falkiewicz B.: Biodegradation of Silicones. Biopolymers, **9**, 539-568 (2003).

[27] Backman S., Björling G., Johansson U. B., Lysdahl M., Markström A., Schedin U., Aune R. E., Frostell C., Karlsson S.: Material wear of polymeric tracheostomy tubes: A six-month study. The Laryngoscope, **119**, 657-664 (2009).

[28] Kaali P., Strömberg E., Aune R. E., Czel G., Momcilovic D.Karlsson S.: Antimicrobial properties of Ag+ loaded zeolite polyester polyurethane and silicone rubber and long-term properties after exposure to in-vitro ageing. Polymer Degradation and Stability, **95**, 1456-1465 (2010).

[29] Santerre J. P., Woodhouse K., Laroche G., Labow R. S.: Understanding the biodegradation of polyurethanes: From classical implants to tissue engineering materials. Biomaterials, **26**, 7457-7470 (2005).

[30] Frautschi J. R., Chinn J. A., Phillips Jr R. E., Zhao Q. H., Anderson J. M., Joshi R., Levy R. J.: Degradation of polyurethanes in vitro and in vitro: comparison of different models. Colloids and Surfaces B: Biointerfaces, **1**, 305-313 (1993).

[31] Wiggins M. J., Wilkoff B., Anderson J. M., Hiltner A.: Biodegradation of polyether polyurethane inner insulation in bipolar pacemaker leads. Journal of Biomedical Materials Research, **58**, 302-307 (2001).

[32] Christenson E. M., Patel S., Anderson J. M., Hiltner A.: Enzymatic degradation of poly(ether urethane) and poly(carbonate urethane) by cholesterol esterase. Biomaterials, **27**, 3920-3926 (2006).

[33] Duguay D. G., Labow R. S., Santerre J. P., McLean D. D.: Development of a mathematical model describing the enzymatic degradation of biomedical polyurethanes. 1. Background, rationale and model formulation. Polymer Degradation and Stability, **47**, 229-249 (1995).

[34] Santerre J. P., Duguay Daniel G., Labow Rosalind S.Brash John L.: Interactions of Hydrolytic Enzymes at an Aqueous Polyurethane, in ´Proteins at Interfaces´, American Chemical Society, **602**, 352-370 (1995).

[35] Santerre J. P., Labow R. S., Adams G. A.: Enzyme-biomaterial interactions: Effect of biosystems on degradation of polyurethanes. Journal of Biomedical Materials Research, **27**, 97-109 (1993).

[36] Guignot C., Betz N., Legendre B., Le Moel A., Yagoubi N.: Degradation of segmented poly(etherurethane) Tecoflex® induced by electron beam irradiation: Characterization and evaluation. Nuclear Instruments and Methods in Physics Research Section B: Beam Interactions with Materials and Atoms, **185**, 100-107 (2001).

[37] Mrad O., Saunier J., Aymes Chodur C., Rosilio V., Agnely F., Aubert P., Vigneron J., Etcheberry A., Yagoubi N.: A comparison of plasma and electron beam-sterilization of PU catheters. Radiation Physics and Chemistry, **79**, 93-103 (2009).

[38] Mrad O., Saunier J., Chodur C. A., Agnely F., Yagoubi N.: Influence of electron beam sterilization on polymers when incubated in different media. Journal of Applied Polymer Science, **111**, 3113-3120 (2009).

[39] Ravat B., Grivet M., Chambaudet A.: Evolution of the degradation and oxidation of polyurethane versus the electron irradiation parameters: Fluence, flux and temperature. Nuclear Instruments and Methods in Physics Research Section B: Beam Interactions with Materials and Atoms, **179**, 243-248 (2001).

[40] Ravat B., Grivet M., Grohens Y., Chambaudet A.: Electron irradiation of polyesterurethane: study of chemical and structural modifications using FTIR, UV spectroscopy and GPC. Radiation Measurements, **34**, 31-36 (2001).

[41] Haugen H. J., Brunner M., Pellkofer F., Aigner J., Will J., Wintermantel E.: Effect of different -irradiation doses on cytotoxicity and material properties of porous polyether-urethane polymer. Journal of Biomedical Materials Research Part B: Applied Biomaterials, **80B**, 415-423 (2007).

[42] Abraham G. A., Frontini P., Cuadrado T.: Physical and mechanical behavior of sterilized biomedical segmented polyurethanes. Journal of Applied Polymer Science, **65**, 1193-1203 (1997).

[43] Burgos N., Jiménez A.: Degradation of poly(vinyl chloride) plasticized with non-phthalate plasticizers under sterilization conditions. Polymer Degradation and Stability, **94**, 1473-1478 (2009).

[44] Gilding D. K., Reed A. M., Baskett S. A.: Ethylene oxide sterilization: effect of polymer structure and sterilization conditions on residue levels. Biomaterials, **1**, 145-148 (1980).

[45] Lucas A. D., Merritt K., Hitchins V. M., Woods T. O., McNamee S. G., Lyle D. B., Brown S. A.: Residual ethylene oxide in medical devices and device material. Journal of Biomedical Materials Research Part B: Applied Biomaterials, **66B**, 548-552 (2003).

[46] Bolt H. M.: Carcinogenicity and Genotoxicity of Ethylene Oxide: New Aspects and Recent Advances. Critical Reviews in Toxicology, **30**, 595-608 (2000).

[47] MacNeil J. R., Glaser Z. R.: Comparison of health care-based sterilization technologies: safety, efficacy and economics. J Healthcare Safety Compliance Infect Control, 91-106 (1997).

[48] Kumon H., Hashimoto H., Nishimura M., Monden K., Ono N.: Catheter-associated urinary tract infections: impact of catheter materials on their management. International Journal of Antimicrobial Agents, **17**, 311-316 (2001).

[49] Schierholz J. M., Lucas L. J., Rumpc A., Pulverer G.: Efficacy of silver-coated medical devices. Journal of Hospital Infection, **40**, 257-262 (1998).

[50] Böswald M., Mende K., Bernschneider W., Bonakdar S., Ruder H., Kissler H., Sieber E., Guggenbichler J. P.: Biocompatibility testing of a new silver-impregnated catheter *in vivo*. Infection, **27**, S38-S42 (1999).

[51] Paterson D. L., Bach A., Maury E., Offenstadt G., Yasukawa T., Fujita Y., Sari A., Darouiche R. O., Raad I. I.: Antimicrobial-Impregnated Central Venous Catheters. New England Journal of Medicine, **340**, 1761-1762 (1999).

[52] Walder B., Pittet D., Tramer M.: Prevention of bloodstream infections with central venous catheters treated with anti-infective agents depends on catheter type and insertion time: evidence from a meta-analysis. Infection Control and Hospital Epidemiology, **23**, 748-756 (2002).

[53] Kubey W., Luneburg P., Ericson S., Brown J., Holmes C. J., *A* longitudinal in vitro antimicrobial evaluation of two silver polymer surface treatments for peritoneal dialysis catheters, in Advances in peritoneal dialysis. Conference on Peritoneal, 1995.

[54] Castellano J. J., Shafii S. M., Ko F., Donate G., Wright T. E., Mannari R. J., Payne W. G., Smith D. J., Robson M. C.: Comparative evaluation of silver-containing antimicrobial dressings and drugs. International Wound Journal, **4**, 114-122 (2007).

[55] Ip M., Lui S. L., Poon V. K. M., Lung I., Burd A.: Antimicrobial activities of silver dressings: an in vitro comparison. Journal of Medical Microbiology, **55**, 59-63 (2006).

[56] Kwan K. L., Fontecchio S. A.: Use of silver-hydrogel urinary catheters on the incidence of catheter-associated urinary tract infections in hospitalized patients. American Journal of Infection Control, **30**, 221-225 (2002).

[57] Johnson J. R., Kuskowski M. A., Wilt T. J.: Systematic Review: Antimicrobial Urinary Catheters To Prevent Catheter-Associated Urinary Tract Infection in Hospitalized Patients. Annals of Internal Medicine, **144**, 116-126 (2006).

[58] Chopra I.: The increasing use of silver-based products as antimicrobial agents: a useful development or a cause for concern? Journal of Antimicrobial Chemotherapy, **59**, 587-590 (2007).

[59] Auerbach S. M., Carrado K. A., Dutta P. K.: Handbook of zeolite science and technologyNew York: Marcel Dekker Inc. (2003).

[60] Mumpton F. A.: La roca magica: Uses of natural zeolites in agriculture and industry. Proceedings of the National Academy of Sciences of the United States of America, **96**, 3463-3470 (1999).

[61] Woinarski A. Z., Stevens G. W., Snape I.: A Natural Zeolite Permeable Reactive Barrier to Treat Heavy-Metal Contaminated Waters in Antarctica: Kinetic and Fixed-bed Studies. Process Safety and Environmental Protection, **84**, 109-116 (2006).

[62] Erdem E., Karapinar N., Donat R.: The removal of heavy metal cations by natural zeolites. Journal of Colloid and Interface Science, **280**, 309-314 (2004).

[63] Chojnacki A., Chojnacka K., Hoffmann J., Gurecki H.: The application of natural zeolites for mercury removal: from laboratory tests to industrial scale. Minerals Engineering, **17**, 933-937 (2004).

[64] Papaioannou D., Katsoulos P. D., Panousis N., Karatzias H.: The role of natural and synthetic zeolites as feed additives on the prevention and/or the treatment of certain farm animal diseases: A review. Microporous and Mesoporous Materials, **84**, 161-170 (2005).

[65] Flowers J. L., Lonky S. A., Deitsch E. J.: Clinical evidence supporting the use of an activated clinoptilolite suspension as an agent to increase urinary excretion of toxic heavy metals. Nutrition and Dietary Supplements, **1**, 11-18 (2009).

[66] Inoue Y., Kanzaki Y.: The mechanism of antibacterial activity of silver-loaded zeolite. Journal of Inorganic Biochemistry, **67**, 377-377 (1997).

[67] Fang M., Chen J. H., Xu X. L., Yang P. H., Hildebrand H. F.: Antibacterial activities of inorganic agents on six bacteria associated with oral infections by two susceptibility tests. International Journal of Antimicrobial Agents, **27**, 513-517 (2006).

[68] Zhang Y., Zhong S., Zhang M., Lin Y.: Antibacterial activity of silver-loaded zeolite A prepared by a fast microwave-loading method. Journal of Materials Science, **44**, 457-462 (2009).

[69] Kawahara K., Tsuruda K., Morishita M., Uchida M.: Antibacterial effect of silver-zeolite on oral bacteria under anaerobic conditions. Dental Materials, **16**, 452-455 (2000).

[70] Inoue Y., Hoshino M., Takahashi H., Noguchi T., Murata T., Kanzaki Y., Hamashima H., Sasatsu M.: Bactericidal activity of Ag-zeolite mediated by reactive oxygen species under aerated conditions. Journal of Inorganic Biochemistry, **92**, 37-42 (2002).

[71] Pehlivan H., Balköse D., Ülkü S., Tihminlioglu F.: Characterization of pure and silver exchanged natural zeolite filled polypropylene composite films. Composites Science and Technology, **65**, 2049-2058 (2005).

[72] Kam K., Aksoy E. A., Akata B., Hasirci N., Baç N.: Preparation and characterization of

antibacterial zeolite-polyurethane composites. Journal of Applied Polymer Science, **110**, 2854-2861 (2008).

[73] Cho Y. H., Lee S. J., Lee J. Y., Kim S. W., Lee C. B., Lee W. Y., Yoon M. S.: Antibacterial effect of intraprostatic zinc injection in a rat model of chronic bacterial prostatitis. International Journal of Antimicrobial Agents, **19**, 576-582 (2002).

[74] Boyd D., Li H., Tanner D., Towler M., Wall J.: The antibacterial effects of zinc ion migration from zinc-based glass polyalkenoate cements. Journal of Materials Science: Materials in Medicine, **17**, 489-494 (2006).

[75] Faundez G., Troncoso M., Navarrete P., Figueroa G.: Antimicrobial activity of copper surfaces against suspensions of Salmonella enterica and Campylobacter jejuni. BMC Microbiology, **4**, 19 (2004).

[76] Top A., Ülkü S.: Silver, zinc, and copper exchange in a Na-clinoptilolite and resulting effect on antibacterial activity. Applied Clay Science, **27**, 13-19 (2004).

[77] Chernyavskaya A., Loginova N., Polozov G., Shadyro O., Sheryakov A., Bondarenko E.: Synthesis and antimicrobial activity of silver(I) and copper(II) complexes with 2-(4,6-di-tert-butyl-2,3-dihydroxyphenylsulfanyl) acetic acid. Pharmaceutical Chemistry Journal, **40**, 413-415 (2006).

[78] Jeong S., Yeo S., Yi S.: The effect of filler particle size on the antibacterial properties of compounded polymer/silver fibers. Journal of Materials Science, **40**, 5407-5411 (2005).

[79] Schmidt G., Malwitz M. M.: Properties of polymer-nanoparticle composites. Current Opinion in Colloid & Interface Science, **8**, 103-108 (2003).

[80] Pal S., Tak Y. K., Song J. M.: Does the Antibacterial Activity of Silver Nanoparticles Depend on the Shape of the Nanoparticle? A Study of the Gram-Negative Bacterium Escherichia coli. Applied and Environmental Microbiology, **73**, 1712-1720 (2007).

[81] Dirix Y., Bastiaansen C., Caseri W., Smith P.: Preparation, structure and properties of uniaxially oriented polyethylene-silver nanocomposites. Journal of Materials Science, **34**, 3859-3866 (1999).

[82] Akamatsu K., Takei S., Mizuhata M., Kajinami A., Deki S., Takeoka S., Fujii M., Hayashi S., Yamamoto K.: Preparation and characterization of polymer thin films containing silver and silver sulfide nanoparticles. Thin Solid Films, **359**, 55-60 (2000).

[83] Babu R., Zhang J., Beckman E. J., Virji M., Pasculle W. A., Wells A.: Antimicrobial activities of silver used as a polymerization catalyst for a wound-healing matrix Biomaterials, **27**, 4304-4314 (2006).

[84] Mahapatra S. S., Karak N.: Silver nanoparticle in hyperbranched polyamine: Synthesis, characterization and antibacterial activity. Materials Chemistry and Physics, **112**, 1114-1119 (2008).

[85] Sambhy V., MacBride M. M., Peterson B. R., Sen A.: Silver Bromide Nanoparticle/Polymer Composites; Dual Action Tunable Antimicrobial Materials. Journal of the American Chemical Society, **128**, 9798-9808 (2006).

[86] Kam K., Aksoy E. A., Akata B., Hasirci N., Baç N.: Preparation and characterization of antibacterial zeolite-polyurethane composites. Journal of Applied Polymer Science, **110**, 2854-2861 (2008).

[87] Pehlivan H., Balköse D., Ülkü S., Tihminlioglu F.: Characterization of pure and silver exchanged natural zeolite filled polypropylene composite films. Composites Science Technology, **65**, 2049-2058 (2005).

[88] Bjorling G., Axelsson S., Johansson U. B., Lysdahl M., Markstrom A., Schedin U., Aune R. E., Frostell C., Karlsson S.: Clinical Use and Material Wear of Polymeric Tracheostomy Tubes. Laryngoscope, **9**, 1552-1559 (2007).

[89] Axelsson S.: Corrosive and Chemical Degradation by Biofilms on Bioimplants, in Department of Fibre and Polymertechnology, Royal Institute of Technology: Stockholm (2005).

[90] Herting G., Odnevall Wallinder I., Leygraf C.: Metal release from various grades of stainless steel exposed to synthetic body fluids. Corrosion Science, **49**, 103-111 (2007).

[91] Midander K., Wallinder I. O., Leygraf C.: In vitro studies of copper release from powder particles in synthetic biological media. Environmental Pollution, **145**, 51-59 (2007).

[92] Murgasova R., Brantley E. L., Hercules D. M., Nefzger H.: Characterization of Polyester-Polyurethane Soft and Hard Blocks by a Combination of MALDI, SEC, and Chemical Degradation. Macromolecules, **35**, 8338-8345 (2002).

[93] Mehl J. T., Murgasova R., Dong X., Hercules D. M., Nefzger H.: Characterization of Polyether and Polyester Polyurethane Soft Blocks Using MALDI Mass Spectrometry. Analytical Chemistry, **72**, 2490-2498 (2000).

[94] Hunt S. M., George G. A.: Characterization of siloxane residues from polydimethylsiloxane elastomers by MALDI-TOF-MS. Polymer International, **49**, 633-635 (2000).

[95] Slatser J. C.: Atomic Radii in Crystals. Journal of Chemical Physics, **41**, 3199-3205 (1964).

[96] Shannon R. H.: Revised effective ionic radii and systematic studies of interatomic distances in halides and chalcogenides. Acta Crystallographica Section A: Foundations of Crystallography, **32**, 751-761 (1976).

[97] Kielland J.: Individual activity coefficients of ions in aqueous solutions Journal of American Chemical Society, **59**, 1675-1678 (1937).

[98] Adams J. M., Haselden D. A., Hewat A. W.: The structure of dehydrated Na zeolite A by neutron profile refinement. Journal of Solid State Chemistry, **44**, 254-253 (1982).

[99] Gellens L. R., Mortier W. J., Schoonheyd R. A., Uytterhoeven J. B.: The nature of charged silver clusters in dehydrated zeolites of type A. Journal of Physical Chemistry, **85**, 2783-2788 (1981).

[100] Lee H. S., Seff K.: Redox reactions of copper in zeolite A. Four crystal structures of vacuum-desolvated copper-exchanged zeolite A. Journal of Physical Chemistry, **85**, 397-410 (1981).

[101] Denyer S. P., Hanlon G. W., Davies M. C.: Mechanisms of Microbial Adherence, in ´Mechanisms of Microbial Adherence´ (eds.: Denyer S. P., Gorman S. P., and Sussman M.) Blackwell Scientific Publications, Cambridge, 13-28 (1993).

[102] Dickinson R. B., Ruta A. G., Treusdal S. E.: Physicochemical Basis of Bacterial Adhesion to Biomaterial Surfaces, in ´Physicochemical Basis of Bacterial Adhesion to Biomaterial Surfaces´ (ed.: Sawan S. and Manivannan G.) Technomic Publishing Company, Inc., Lancaster, 69-81 (2000).

[103] Bodas D., Khan-Malek C.: Hydrophilization and hydrophobic recovery of PDMS by oxygen plasma and chemical treatment- An SEM investigation. Sensors and Actuators, **127**, 368-373 (2007).

[104] Kumagai S., Yoshimura N.: Hydrophobic Transfers of RTV Silicone Rubber Aged in Single and Multiple Environmental Stresses and the Behaviour of LMW Silicone Fluid. IEEE Transactions on Power Delivery, **18**, 506-516 (2003).

[105] Hillborg H., Gedde U. W.: Hydrophobicity Changes in Silicone Rubbers. IEEE Transactions on Power Delivery, **5**, 703-717 (1999).

[106] Zhu Y., Otsubo M., Honda C., Tanaka S.: Loss and recovery in hydrophobicity of silicone rubber exposed to corona discharge. Polymer Degradation and Stability, **91**, 1448-1454 (2006).

[107] Kim J., Chaudry M. K., Owen M. J.: Modeling hydrophobic recovery of electrically discharged polydimethyilsiloxane elastomers. Journal of Colloid and Interface Science, 364-375 (2006).

[108] Tan J., Chao Y. J., Li X., Van Zee J. W.: Degradation of silicone rubber under compression in a simulated PEM fuel cell environment. Journal of Power Sources, **172**, 782-789 (2007).

[109] Socrates G.: Organic Silicone Compounds, John Wiley and Sons Ltd., Chichester, 239-246 (2001).

[110] Gorur R. S., Karady G. G., Jagota A., Shah M., Yates A. M.: Aging in silicone rubber used for outdoor insulation. IEEE Transactions on Power Delivery, **7**, 525-538 (1992).

[111] Gaboury S. R., Urban M. W.: Quantitative analysis of the Si-H groups formed on poly(dimethylsiloxane) surfaces: an ATR FTi.r. approach. Polymer, **33**, 5085-5089 (1992).

[112] Mendelovici E., Frost R. L., Kloprogge J. T.: Modification of Chrysotile Surface by Organosilanes: An IR-Photoacoustic Spectroscopy Study. Journal of Colloid and Interface Science, **238**, 273-278 (2001).

[113] Bosch A., Serra D., Prieto C., Schmitt J., Naumann D., Yantorno O.: Characterization of Bordetella pertussis growing as biofilm by chemical analysis and FT-IR spectroscopy Applied Microbiology and Biotechnology, **71**, 736-747 (2006).

[114] Bosch A., Miñán A., Vescina C., Degrossi J., Gatti B., Montanaro P., Messina M., Franco M., Vay C., Schmitt J., Naumann D., Yantorno O.: Fourier Transform Infrared Spectroscopy for Rapid Identification of Nonfermenting Gram-Negative Bacteria Isolated from Sputum Samples from Cystic Fibrosis Patients. Journal of Clinical Microbiology, **46**, 2535-2546 (2008).

[115] Schmitt J., Flemming H. C.: FTIR-spectroscopy in microbial and material analysis. International Biodeterioration & Biodegradation, **41**, 1-11 (1998).

[116] Donlan R. M., Piede J. A., Heyes C. D., Sanii L., Murga R., Edmonds P., El-Sayed I., El-Sayed M. A.: Model System for Growing and Quantifying Streptococcus pneumoniae Biofilms In Situ and in Real Time. Applied and Environment Microbiology, **70**, 4980-4988 (2004).

[117] Helm D., Naumann D.: Identification of some bacterial cell components by FT-IR spectroscopy. FEMS Microbiology Letters, **126**, 75-79 (1995).

[118] Wallström S., Karlsson S.: Biofilms on silicone rubber insulators; microbial composition and diagnostics of removal by use of ESEM/EDS: Composition of biofilms infecting silicone rubber insulators. Polymer Degradation and Stability, **85**, 841-846 (2004).

[119] Graiver D., Farminer K. W., Narayan R.: A Review of the Fate and Effects of Silicones in the Environment. Journal of Polymers and the Environment, **11**, 129-136 (2003).

[120] Brinker C. J., Scherer G. W.: Sol-Gel Science: The Physics and Chemistry of Sol-Gel Processing, New York: Academic Press Inc. (1990).

[121] Rehman I., Andrews E. H., Smith R.: In vitro degradation of poly(ester-urethanes) for biomedical applications. Journal of Materials Science: Materials in Medicine, **7**, 17-20 (1996).

[122] McCarthy S. J., Meijs G. F., Mitchell N., Gunatillake P. A., Heath G., Brandwood A.Schindhelm K.: In-vivo degradation of polyurethanes: transmission-FTIR microscopic characterization of polyurethanes sectioned by cryomicrotomy. Biomaterials, **18**, 1387-1409 (1997).

[123] Frautschi J. R., Chinn J. A., Phillips R. E., Zhao Q. H., Anderson J. M., Joshi R., Levy R. J.: Degradation of polyurethanes in vitro and in vitro: comparison of different models. Colloids and Surfaces B: Biointerfaces, **1**, 305-313 (1993).

[124] Guignot C., Betz N., Legendre B., Le Moel A., Yagoubi N.: Degradation of segmented poly(etherurethane) Tecoflex® induced by electron beam irradiation: Characterization and evaluation. Nuclear Instruments & Methods in Physics Research, Section B: Beam Interactions with Materials and Atoms, **185**, 100-107 (2001).

[125] Sarkar D., Lopina S. T.: Oxidative and enzymatic degradations of l-tyrosine based polyurethanes. Polymer Degradation and Stability, **92**, 1994-2004 (2007).

[126] Skaja A., Fernando D., Croll S.: Mechanical property changes and degradation during accelerated weathering of polyester-urethane coatings. Journal of Coatings Technology and Research, **3**, 41-51 (2006).

[127] Kaali P., Momcilovic D., Markström A., Aune R., Czel G., Karlsson S.: Degradation of biomedical polydimethylsiloxanes during exposure to *in vivo* biofilm environment monitored by FE-SEM, ATR-FTIR, and MALDI-TOF MS. Journal of Applied Polymer Science, **115**, 802-810).

[128] Chen H., He M.: Quantitation of synthetic polymers using an internal standard by matrix-assisted laser desorption/ionization time-of-flight mass spectrometry. Journal of the American Society for Mass Spectrometry, **16**, 100-106 (2005).

[129] Okuno S., Wada Y., Arakawa R.: Quantitative analysis of polypropylenglycol mixtures by desorptio/ionization on porous silicon mass spectrometry. International Journal of Mass Spectrometry and Ion Processes, **241**, 43-48 (2005).

[130] Chen H., He M., Pei J., He H.: Quantitative Analysis of Synthetic Polymers Using Matrix-Assisted Laser Desorption/Ionization Time-of-Flight Mass Spectrometry. Analytical Chemistry, **75**, 6531-6535 (2003).